



An Expanded Local Variance Gamma Model

P. Carr¹ · A. Itkin¹

Accepted: 16 May 2020

© Springer Science+Business Media, LLC, part of Springer Nature 2020

Abstract

The paper proposes an expanded version of the Local Variance Gamma model of Carr and Nadtochiy by adding drift to the governing underlying process. Still in this new model it is possible to derive an ordinary differential equation for the option price which plays a role of Dupire's equation for the standard local volatility model. It is shown how calibration of multiple smiles (the whole local volatility surface) can be done in such a case. Further, assuming the local variance to be a piecewise linear function of strike and piecewise constant function of time this ODE is solved in closed form in terms of Confluent hypergeometric functions. Calibration of the model to market smiles does not require solving any optimization problem and, in contrast, can be done term-by-term by solving a system of non-linear algebraic equations for each maturity. This is much faster as compared with calibration which requires solving the Dupire PDE.

Keywords Local volatility · Stochastic clock · Gamma distribution · Piecewise linear variance · Variance Gamma process · Closed form solution · Fast calibration · No-arbitrage

1 Introduction

Local volatility model was introduced by Dupire (1994) and Derman and Kani (1994) as a natural extension of the celebrated Black–Scholes model to take into account an existence of option smile. It is able to exactly replicate the local volatility function $\sigma(T, K)$ where K, T are the option strike and time to maturity, at given pairs (T, K) where the European options prices or their implied volatilities are known. This process is called calibration of the local volatility (or, alternatively, implied

✉ A. Itkin
aitkin@nyu.edu

P. Carr
petercarr@nyu.edu

¹ Tandon School of Engineering, New York University, 12 Metro Tech Center, 26th Floor, Brooklyn, NY 11201, USA

volatility) surface. Various approaches to solving this important problem were proposed, see, e.g., survey in Itkin and Lipton (2018) and references therein.

As mentioned in Itkin and Lipton (2018), there are two main approaches to solving the calibration problem. The first approach relies on some parametric or non-parametric regression to construct a continuous implied volatility (IV) surface matching the given market quotes. Then the corresponding local volatility surface can be found via the well-known Dupire's formula, see, e.g., Itkin (2015) and references therein.

The second approach relies on the direct solution of the Dupire equation using either analytical or numerical methods. The advantage of this approach is that it guarantees no-arbitrage¹. However, the problem of the direct solution can be ill-posed (Coleman et al. 2001), and is rather computationally expensive. For instance, in Itkin and Lipton (2018) the Dupire equation (a partial differential equation (PDE) of the parabolic type) is solved by i) first using the Laplace-Carson transform, and ii) then applying various transformations to obtain a closed form solution of the transformed equation in terms of Kummer hypergeometric functions. Still, it requires an inverse Laplace transform to obtain the final solution.

With the second approach in use one also has to make an assumption about the behavior of the local/implied volatility surface at strikes and maturities where the market quotes are not known. Usually, by a tractability argument the corresponding local variance is seen either piecewise constant (Lipton and Sepp 2011), or piecewise linear (Itkin and Lipton 2018) in the log-strike space, and piecewise constant in the time to maturity space².

To improve computational efficiency of calibration, an important step is made in Carr and Nadtochiy (2017) where Local Variance Gamma (LVG) model has been introduced (the first version refers to 2014 and can be found in Carr and Nadtochiy (2014)). This model assumes that the risk-neutral process for the underlying futures price is a pure jump Markov martingale, and that European option prices are given at a continuum of strikes and at one or more maturities. The authors construct a time-homogeneous process which meets a single smile and a piecewise time-homogeneous process, which can meet multiple smiles. However, in contrast to e.g., Itkin and Lipton (2018), their construction leads not to a PDE, but to a partial differential difference equation (PDDE), which permits both explicit calibration and fast numerical valuation. In particular, it does not require application of any optimization methods, rather just a root solver. Therefore, as compared with the calibration of the local volatility model, computation of the objective function for the LVG at requires just solving an algebraic system of equations, while for the local volatility model it requires solving the Dupire PDE (for instance, using the inverse Laplace transform, see Itkin and Lipton (2018)). In Carr and Nadtochiy (2017) this model is used to calibrate the local volatility surface assuming its piecewise constant structure in the strike space.

¹ But only if an analytical or numerical method in use does preserve no-arbitrage. This includes various interpolations, etc.

² See, however, comments in Itkin and Lipton (2018) about their assumptions.

One of the potential criticism of this calibration method is the fact that the resulting local volatility function has a finite number of discontinuities. So it would be advantaged to relax the piecewise constant behavior of the surface. This is similar to how Itkin and Lipton (2018) was developed to overcome the same problem as compared with Lipton and Sepp (2011).

On this way, recently Falck and Deryabin (2017) applied the LVG model to the FX options market where usually option prices are quoted only at five strikes. They assumed that the local volatility function is continuous, piecewise linear in the four inner strike subintervals and constant in the outer subintervals. A closed form solution of the PDDE derived in Carr and Nadtochiy (2014)) is obtained with this parametrization, and calibration of some volatility smiles is provided. Still, to calibrate the model the authors rely on a residual minimization by using a least-square approach. So, despite an improved version of the LVG model is used, computational efficiency of this method is not perfect.

Another remark of Carr and Nadtochiy (2017) is about the limitation that the risk-neutral price process of the underlying is assumed to be a martingale, i.e. the main driving process in (1) doesn't have a drift. However, the drift may not be negligible. If the drift is deterministic, e.g. when the interest rate and dividends are deterministic, and the drift is a deterministic function of them, the calibration problem can be reduced to the driftless case by discounting, but this assumption might be inconsistent with the market. Therefore, an expansion of the proposed model that allows for a non-zero and stochastic drift is very desirable. In particular, it would be interesting to expand the LVG model to a risk-neutral price process obtained by stochastic time change of a drifted diffusion. In this way, similar to local Variance Gamma model (Madan et al. 1998), we introduce both stochastic volatility and stochastic drift. This is especially important if instead of, say, the equity options we price the FX options, or eliminate risk-neutral valuation and work under real P measure. Non-zero drift could also come as, e.g., a conventional yield for commodities, or as a compensator for the jump processes if we extend the model to the jump-diffusion processes, etc.

With this in mind, our ultimate goals in this paper are as follows. First, we propose an expanded version of the LVG model by adding drift to the governing underlying process. It turns out that to proceed we need to re-derive and re-think every step in construction proposed in Carr and Nadtochiy (2017). We show that still it is possible to find an ordinary differential equation (ODE) for the option price which plays a role of Dupire's equation for the standard local volatility model, and how calibration of multiple smiles (the whole local volatility surface) can be done in such a case.

We want to underline that the LVG, as well as its extension presented in this paper (ELVG), is actually a stochastic local volatility model. As compared with the classical local volatility model, both LVG and ELVG models have several advantages. First, they are richer in the financial sense. Indeed, it is worth noting that the term "local" in the name of the LVG/ELVG models is a bit confusing. This is because, e.g., the ELVG is constructed by equipping an arithmetic Brownian motion with drift and local volatility by stochastic time change $\Gamma_{X(t)}$. Here Γ_t is a Gamma stochastic variable, and $X(t)$ is a deterministic function of time t . As stochastic change is one of the ways of introducing stochastic volatility, it could be observed that the

LVG/ELVG is actually a local stochastic volatility (LSV) model which combines local and stochastic features of the volatility process. For more information on the LSV models, see Bergomi (2016); Kienitz and Wetterau (2012). So, the approach of Itkin and Lipton (2018) is used in this paper just as a reference and for benchmarking to compare the speed of the methods.

Further, assuming the local variance to be a piecewise linear function of strike and piecewise constant function of time we solve this ODE in closed form in terms of Confluent hypergeometric functions. Calibration of the model to market smiles does not require solving any optimization problem. In contrast, it can be done term-by-term by solving a system of non-linear algebraic equations for each maturity. This is much faster as compared with the classical calibration approach where to construct the objective function the optimizer needs the solution of the Dupire PDE.

The rest of the paper is organized as follows. In Sect. 2 the Expanded Local Variance Gamma model is formulated. In Sect. 3 we derive a forward equation (which is an ordinary differential equation (ODE)) for Put option prices using a homogeneous Bochner subordination approach. Section 4 generalizes this approach by considering the local variance being piece-wise constant in time. In Sect. 5 a closed form solution of the derived ODE is given in terms of Confluent hypergeometric functions. The next section discusses computation of a source term of this ODE which requires a no-arbitrage interpolation. Using the idea of Itkin and Lipton (2018)), we show how to construct non-linear interpolation which provides both no-arbitrage, and a nice tractable representation of the source term, so that all integrals in the source term can be computed in closed form. In Sect. 7 calibration of multiple smiles in our model is discussed in detail. To calibrate a single smile we derive a system of nonlinear algebraic equations for the model parameters, and explain how to obtain a smart guess for their initial values. In Sect. 8 asymptotic solutions of our ODE at extreme values of the model parameters are derived which improve computational accuracy and speed of the numerical solution. Section 9 presents the results of some numerical experiments where calibration of the model to the given market smiles is done term-by-term. The last section concludes.

2 Process

Below where possible we follow the notation of Carr and Nadtochiy (2017).

Let W_t be a \mathbb{Q} standard Brownian motion with time index $t \geq 0$. Consider a stochastic process D_t to be a time-homogeneous diffusion

$$dD_t = \mu D_t dt + \sigma(D_t) dW_t, \quad (1)$$

where the volatility function σ is local and time-homogeneous, and μ is deterministic.

A unique solution to (1) exists if $\sigma(D) : \mathbb{R} \rightarrow \mathbb{R}$ is Lipschitz continuous in D and satisfies growth conditions at infinity. According to (1) we have $D_t \in (-\infty, \infty)$ while $t \in [0, \infty)$. Since D is a time-homogeneous Markov process, its infinitesimal generator \mathcal{A} is given by

$$\mathcal{A}\phi(D) \equiv \left[\mu D \nabla_D + \frac{1}{2} \sigma^2(D) \mathcal{D}_D^2 \right] \phi(D) \quad (2)$$

for all twice differentiable functions ϕ . Here \mathcal{D}_x is a first order differential operator on x . The semigroup of the D process is

$$\mathcal{T}_t^D \phi(D_t) = e^{t\mathcal{A}} \phi(D_t) = \mathbb{E}_{\mathbb{Q}}[\phi(D_t) | D_0 = D], \quad \forall t \geq 0. \quad (3)$$

In the spirit of Variance Gamma model, (Madan and Seneta 1990; Madan et al. 1998) and similar to Carr and Nadtochiy (2017), introduce a new process D_{Γ_t} which is D_t subordinated by the unbiased Gamma clock Γ_t . The density of the unbiased Gamma clock Γ_t at time $t \geq 0$ is

$$\mathbb{Q}\{\Gamma_t \in d\nu\} = \frac{\nu^{m-1} e^{-\nu m/t}}{(t^*)^m \Gamma(m)} d\nu, \quad \nu > 0, \quad m \equiv t/t^*. \quad (4)$$

Here $t^* > 0$ is a free parameter of the process, $\Gamma(x)$ is the Gamma function. It is easy to check that

$$\mathbb{E}_{\mathbb{Q}}[\Gamma_t] = t. \quad (5)$$

Thus, on average the stochastic gamma clock Γ_t runs synchronously with the calendar time t .

As applied to the option pricing problem, we introduce a more complex construction. Namely, consider options written on the underlying process S_t . Without loss of generality and for the sake of clearness let us treat below S_t as the stock price process. Here, in contrast to Carr and Nadtochiy (2017), we don't ignore interest rates r and continuous dividends q assuming them to be deterministic (below for simplicity of presentation we treat them as constants, but this can be easily relaxed). Then, let us define S_t as

$$S_t = D_{\Gamma_{X(t)}}, \quad X(t) = \frac{1 - e^{-(r-q)t}}{r - q}. \quad (6)$$

It is clear that in the limit $r \rightarrow 0$, $q \rightarrow 0$ we have $X(t) = t$, i.e., in this limit our construction coincides with that in Carr and Nadtochiy (2017) who considered a driftless diffusion and assumed $S_t = D_{\Gamma_t}$. Also based on (5)

$$\mathbb{E}_{\mathbb{Q}}[\Gamma_{X(t)}] = X(t). \quad (7)$$

Function $X(t)$ starts at zero, ie, $X(0) = 0$, and is a continuous increasing function of time t . Indeed, if $r - q > 0$, then $X(t)$ is increasing in t on $t \in [0, \infty)$, and at $t \rightarrow \infty$ it tends to constant. The infinite time horizon is not practically important, but for any finite time t function $X(t)$ can be treated as an increasing function in t . If $r - q < 0$, function $X(t)$ is strictly increasing $\forall t \in [0, \infty)$. Thus, $X(t)$ has all properties of a good clock. Accordingly, $\Gamma_{X(t)}$ has all properties of a random time.

Under a risk-neutral measure \mathbb{Q} , the total gain process, including the underlying price appreciation and dividends, after discounting at the risk free rate should

be a martingale, see, e.g., Shreve (1992). This process obeys the following stochastic differential equation

$$d(e^{-rt}S_t e^{qt}) = e^{(q-r)t}[(q-r)S_t dt + dS_t]. \quad (8)$$

Taking an expectation of both parts we obtain

$$\mathbb{E}_{\mathbb{Q}}[d(e^{(q-r)t}S_t)] = e^{(q-r)t}\{(q-r)\mathbb{E}_{\mathbb{Q}}[S_t]dt + d\mathbb{E}_{\mathbb{Q}}[S_t]\}. \quad (9)$$

Observe, that from (6), (1)

$$\mathbb{E}_{\mathbb{Q}}[dS_t] = \mathbb{E}_{\mathbb{Q}}[dD_{\Gamma_{X(t)}}] = \mu\mathbb{E}_{\mathbb{Q}}[D_{\Gamma_{X(t)}}d\Gamma_{X(t)}] + \mathbb{E}_{\mathbb{Q}}[\sigma(D_{\Gamma_{X(t)}})dW_{\Gamma_{X(t)}}] = \mu\mathbb{E}_{\mathbb{Q}}[D_{\Gamma_{X(t)}}d\Gamma_{X(t)}], \quad (10)$$

because the process W_{Γ_t} is a local martingale, see Revuz and Yor (1999), chapter 6. Accordingly, the process $W_{\Gamma_{X(t)}}$ inherits this property from W_{Γ_t} , hence $\mathbb{E}_{\mathbb{Q}}[\sigma(D_{\Gamma_{X(t)}})dW_{\Gamma_{X(t)}}] = 0$.

Further assume that the Gamma process Γ_t is independent of W_t (and, accordingly, $\Gamma_{X(t)}$ is independent of $W_{\Gamma_{X(t)}}$). Then the expectation in the RHS of (10) can be computed, by first conditioning on $\Gamma_{X(t)}$, and then integrating over the distribution of $\Gamma_{X(t)}$ which can be obtained from (4) by replacing t with $X(t)$, i.e.

$$\begin{aligned} \mathbb{E}_{\mathbb{Q}}[D_{\Gamma_{X(t)}}d\Gamma_{X(t)}|S_s] &= \int_0^\infty \mathbb{E}_{\mathbb{Q}}[D_{\Gamma_{X(t)}}d\Gamma_{X(t)}|\Gamma_{X(t)} = \nu] \frac{\nu^{m-1}e^{-\nu m/X(t)}}{(t^*)^m \Gamma(m)} \\ &= \int_0^\infty \mathbb{E}_{\mathbb{Q}}[D_\nu] \frac{\nu^{m-1}e^{-\nu m/X(t)}}{(t^*)^m \Gamma(m)} d\nu, \quad \nu > 0, \quad m \equiv X(t)/t^*. \end{aligned} \quad (11)$$

The find $\mathbb{E}_{\mathbb{Q}}[D_\nu]$ we take into account (1) to obtain

$$d\mathbb{E}_{\mathbb{Q}}[D_\nu] = \mathbb{E}_{\mathbb{Q}}[dD_\nu] = \mathbb{E}_{\mathbb{Q}}[\mu D_\nu d\nu + \sigma(D_\nu)D_\nu dW_\nu] = \mu\mathbb{E}_{\mathbb{Q}}[D_\nu]d\nu. \quad (12)$$

Solving this equation with respect to $y(\nu) = \mathbb{E}_{\mathbb{Q}}[D_\nu|D_s]$, we obtain $\mathbb{E}_{\mathbb{Q}}[D_\nu|D_s] = D_s e^{\mu(\nu-s)}$. Since we condition on time s , it means that $D_s = D_{\Gamma_{X(s)}} = S_s$, and thus $\mathbb{E}_{\mathbb{Q}}[D_\nu|D_s] = S_s e^{\mu(\nu-s)}$.

Further, we substitute this into (11), set the parameter of the Gamma distribution t^* to be $t^* = X(t)$ (so $m = 1$) and integrate to obtain

$$d\mathbb{E}_{\mathbb{Q}}[S_t|S_s] = \mathbb{E}_{\mathbb{Q}}[dS_t|S_s] = \mu\mathbb{E}_{\mathbb{Q}}[D_{\Gamma_{X(t)}}d\Gamma_{X(t)}] = S_s e^{-s\mu} \frac{\mu}{1 - \mu X(t)}. \quad (13)$$

Setting now $m = r - q$ and solving this equation we find

$$\mathbb{E}_{\mathbb{Q}}[S_t|S_s] = S_s(r-q)e^{(q-r)(s-t)}. \quad (14)$$

Substituting (14) and (13) into (9) yields $d(e^{-rt}S_t e^{qt}) = 0$. Thus, if we chose $\mu = r - q$, the right hands part of (8) vanishes, and our discounted stock process with allowance for non-zero interest rates and continuous dividends becomes a martingale. So the proposed construction can be used for option pricing.

This setting can be easily generalized for time-dependent interest rates $r(t)$ and continuous dividends $q(t)$. We leave it for the reader.

The next step is to consider connection between the original and time-changed processes. It is known from Bochner (1949) that the process G_{T_t} defined as

$$dG_t = \sigma^2(G) dW_t$$

is a time-homogeneous Markov process. As the deterministic process μt is also time-homogeneous, the whole process D_t defined in (1) is also a time-homogeneous Markov process. Accordingly, the semigroups T_t^S of S_t and T_t^D of $D_{T_{X(t)}}$ are connected by the Bochner integral

$$T_t^S U(S) = \int_0^\infty T_v^D U(S) \mathbb{Q}\{T_{X(t)} \in dv\}, \quad \forall t \geq 0, \quad (15)$$

where $U(S)$ is a function in the domain of both T_t^D and T_t^S . It can be derived by exploiting the time homogeneity of the D process, conditioning on the gamma time first, and taking into account the independence of T_t and W_t (or $T_{X(t)}$ and $W_{T_{X(t)}}$ in our case).

We set parameter t^* of the gamma clock to $t^* = X(t)$. Then (15) and (4) imply

$$T_t^S U(S) = \int_0^\infty T_v^D U(S) \frac{e^{-v/X(t)}}{X(t)} dv. \quad (16)$$

In what follows for the sake of brevity we will call this model as an Expanded Local Variance Gamma model, or ELVG.

3 Forward Equation for Put Option Prices

Following Carr and Nadtochiy (2017) we interpret the index t of the semigroup T_t^S as the maturity date T of a European claim with the valuation time $t = 0$. Also let the test function $U(S)$ be the payoff of this European claim, ie,

$$U(S_T) = e^{-rT} (K - S_T)^+. \quad (17)$$

Then define

$$P(S_0, T, K) = T_T^S U(S_0) \quad (18)$$

as the European Put value with maturity T at time $t = 0$ in the ELVG model. Similarly

$$P^D(S_0, v, K) = T_v^D U(S_0) \quad (19)$$

would be the European Put value with maturity ν at time $t = 0$ in the model of (1)³. Then the Bochner integral in (16) takes the form

$$P(S, T, K) = \int_0^\infty P^D(S, \nu, K) p e^{-p\nu} d\nu, \quad p \equiv 1/X(T). \quad (20)$$

Thus, $P(S, X(T), K)$ is represented by a Laplace-Carson transform of $P^D(S, \nu, K)$ with p being a parameter of the transform. Note that

$$P(S, 0, K) = P^D(S, 0, K) = U(S). \quad (21)$$

To proceed, we need an analog of the Dupire forward PDE for $P^D(S, \nu, K)$.

3.1 Derivation of the Dupire Forward PDE

Despite this can be done in many different ways, below for the sake of compatibility we do it in the spirit of Carr and Nadtochiy (2017).

First, differentiating (19) by ν with allowance for (3) yields

$$\nabla_\nu P^D(S, \nu, K) = e^{-r\nu} e^{\nu\mathcal{A}} [\mathcal{A} - r] U(S) = e^{-r\nu} \mathbb{E}_Q [\mathcal{A} - r] U(S). \quad (22)$$

We take into account the definition of the generator \mathcal{A} in (2), and also remind that at $t = 0$ we have $D_0 = S_0$. Then (22) transforms to

$$\nabla_\nu P^D(S, \nu, K) = -rP^D(S, \nu, K) + (r - q)S\nabla_S P^D(S, \nu, K) + e^{-r\nu} \frac{1}{2} \mathbb{E}_Q [\sigma^2(S) \nabla_S^2 U(S)]. \quad (23)$$

However, we need to express the forward equation using a pair of independent variables (ν, K) while (22) is derived in terms of (ν, S) . To do this, observe that

$$\begin{aligned} e^{-r\nu} \mathbb{E}_Q [\sigma^2(S) \nabla_S^2 U(S)] &= e^{-r\nu} \mathbb{E}_Q [\sigma^2(S) \delta(K - S)] = e^{-r\nu} \mathbb{E}_Q [\sigma^2(K) \delta(K - S)] \\ &= e^{-r\nu} \mathbb{E}_Q [\sigma^2(K) \nabla_K^2 U(S)] = \sigma^2(K) \nabla_K^2 P^D(S, \nu, K). \end{aligned} \quad (24)$$

where the sifting property of the Dirac delta function $\delta(S - K)$ has been used. Also

$$\begin{aligned} &-rP^D(S, \nu, K) + (r - q)S\nabla_S P^D(S, \nu, K) \\ &= e^{-r\nu} \mathbb{E}_Q \left[-r(K - S)^+ + (r - q)S \frac{\partial(K - S)^+}{\partial S} \right] \\ &= e^{-r\nu} \mathbb{E}_Q \left[-r(K - S)^+ - (r - q)(K - S) \frac{\partial(K - S)^+}{\partial S} + (r - q)K \frac{\partial(K - S)^+}{\partial S} \right] \\ &= e^{-r\nu} \mathbb{E}_Q \left[-r(K - S)^+ + (r - q)(K - S)^+ - (r - q)K \frac{\partial(K - S)^+}{\partial K} \right] \\ &= -qP^D(S, \nu, K) - (r - q)K \nabla_K P^D(S, \nu, K). \end{aligned} \quad (25)$$

³ Below for simplicity of notation we drop the subscript '0' in S_0 .

Therefore, using (24) and (25), (22) could be transformed to

$$\begin{aligned}\nabla_v P^D(S, v, K) &= -qP^D(S, v, K) - (r - q)K\nabla_K P^D(S, v, K) + \frac{1}{2}\sigma^2(K)K^2\nabla_K^2 P^D(S, v, K) \\ &\equiv \mathcal{A}^K P^D(S, v, K), \\ \mathcal{A}^K &= -q - (r - q)K\nabla_K + \frac{1}{2}\sigma^2(K)K^2\nabla_K^2.\end{aligned}\quad (26)$$

This equation looks exactly like the Dupire equation with non-zero interest rates and continuous dividends, see, e.g., Ekström and Tysk (2012) and references therein. Note, that \mathcal{A}^K is also a time-homogeneous generator.

3.2 Forward Partial Divided-Difference Equation

Our final step is to apply the linear differential operator \mathcal{A}^K defined in (26) to both parts of (20). Using time-homogeneity of D_t and, again, the Dupire equation (26), we obtain

$$\begin{aligned}&-qP(S, T, K) - (r - q)K\nabla_K P(S, T, K) + \frac{1}{2}\sigma^2(K)\nabla_K^2 P(S, T, K) \\ &= \int_0^\infty pe^{-pv} \left[-qP^D(S, v, K) - (r - q)K\nabla_K P^D(S, v, K) + \frac{1}{2}\sigma^2(K)\nabla_K^2 P^D(S, v, K) \right] dv \\ &= \int_0^\infty pe^{-pv} \nabla_v P^D(S, v, K) dv = -pP^D(S, 0, K) + p \int_0^\infty P^D(S, v, K) pe^{-pv} dv \\ &= p[P(S, T, K) - P^D(S, 0, K)] = p[P(S, T, K) - P(S, 0, K)],\end{aligned}\quad (27)$$

where in the last line (21) was taken into account.

Thus, finally $P(S, T, K)$ solves the following problem

$$\begin{aligned}&-qP(S, T, K) - (r - q)K\nabla_K P(S, T, K) + \frac{1}{2}\sigma^2(K)\nabla_K^2 P(S, T, K) \\ &= \frac{P(S, T, K) - P(S, 0, K)}{X(T)}, \quad P(S, 0, K) = (K - S)^+.\end{aligned}\quad (28)$$

At $r = q = 0$ this equation translates to the corresponding equation in Carr and Nadtochiy (2017). In contrast to the Dupire equation which belongs to the class of PDE, (28) is an ODE, or, more precisely, a partial divided-difference equation (PDDE), since the derivative in time in the right hands part is now replaced by a divided difference. In the form of an ODE it reads

$$\left[\frac{1}{2}\sigma^2(K)\nabla_K^2 - (r - q)K\nabla_K - \left(q + \frac{1}{X(T)} \right) \right] P(S, T, K) = -\frac{P(S, 0, K)}{X(T)}. \quad (29)$$

This equation could be solved analytically for some particular forms of the local volatility function $\sigma(K)$ which are considered later in this paper. Also in the same way a similar equation could be derived for the Call option price $C_0(S, T, K)$ which reads

$$\left[\frac{1}{2} \sigma^2(K) \nabla_K^2 + (r - q) K \nabla_K - \left(q + \frac{1}{X(T)} \right) \right] C_0(S, T, K) = - \frac{C_0(S, 0, K)}{X(T)}, \quad (30)$$

$$C_0(S, 0, K) = (S - K)^+.$$

Solving (29) or (30) provides the way to determine $\sigma(K)$ given market quotes of Call and Put options with maturity T . However, this allows calibration of just a single term. Calibration of the whole local volatility surface, in principle, could be done term-by-term (because of the time-homogeneity assumption) if (29), (30) could be generalized to this case. We consider this in the following section.

4 Local Variance Piece-Wise Constant in Time

To address calibration of multiple smiles, we need to relax some assumptions about time-homogeneity of the process D_t defined in (1). This includes several steps which are described below in more detail.

4.1 Local Variance

Here we assume that the local variance $\sigma(D_t)$ is no more time-homogeneous, but a piece-wise constant function of time $\sigma(D_t, t)$.

Let T_1, T_2, \dots, T_M be the time points at which the variance rate $\sigma^2(D_t)$ jumps deterministically. In other words, at the interval $t \in [T_0, T_1)$, the variance rate is $\sigma_0^2(D_t)$, at $t \in [T_1, T_2)$ it is $\sigma_1^2(D_t)$, etc. This can be also represented as

$$\sigma^2(D_t, t) = \sum_{i=0}^M \sigma_i^2(D_t) w_i(t),$$

$$w_i(t) \equiv \mathbf{1}_{t-T_i} - \mathbf{1}_{t-T_{i+1}}, \quad i = 0, \dots, M, \quad T_0 = 0, \quad T_{M+1} = \infty, \quad \mathbf{1}_x = \begin{cases} 1, & x \geq 0 \\ 0, & x < 0. \end{cases} \quad (31)$$

Note, that

$$\sum_{i=0}^M w_i(t) = \mathbf{1}_t - \mathbf{1}_{t-\infty} = 1, \quad \forall t \geq 0.$$

Therefore, in case when all $\sigma_i^2(D_t)$ are equal, ie, independent on index i , (31) reduces to the case considered in the previous sections.

It is important to notice that our construction implies that the volatility $\sigma(D_t)$ jumps as a function of time at the calendar times T_0, T_1, \dots, T_M , and not at the business times ν determined by the gamma clock. Otherwise, the volatility function would change at random (business) times which means it is stochastic. But this definitely lies out of scope of our model. Therefore, we need to change (31) to

$$\sigma^2(D_{\Gamma_{X(t)}}, \Gamma_{X(t)}) = \sum_{i=0}^M \sigma_i^2(D_i) \bar{w}_i(\mathbb{E}_{\mathbb{Q}}(\Gamma_{X(t)})), \quad (32)$$

$$\begin{aligned} \bar{w}_i(t) &= \mathbf{1}_{X^{-1}(t)-T_i} - \mathbf{1}_{X^{-1}(t)-T_{i+1}}, \quad i = 0, \dots, M, \\ X^{-1}(t) &= \frac{1}{q-r} \log [1 - (r-q)t]. \end{aligned} \quad (33)$$

Hence, when using (6) we have

$$\sigma^2(D_t, t) \Big|_{t=\Gamma_{X(t)}} = \sum_{i=0}^M \sigma_i^2(D_i) \bar{w}_i(X(t)) = \sum_{i=0}^M \sigma_i^2(D_i) w_i(t). \quad (34)$$

Accordingly, if the calendar time t belongs to the interval $T_0 \leq t < T_1$, the infinitesimal generator \mathcal{A} of the semigroup \mathcal{T}_v^D is a function of $\sigma(D_t)$ (and not on $\sigma(D_v)$). As at $T_0 \leq t < T_1$ we assume $\sigma(D) = \sigma_0(D)$, i.e., is constant in time, it doesn't depend of v . Thus, \mathcal{A} (which for this interval of time we will denote as \mathcal{A}_0) is still time-homogeneous.

Similarly, one can see, that for $T_1 \leq t < T_2$ the infinitesimal generator \mathcal{A}_1 of the semigroup \mathcal{T}_v^D is also time-homogeneous and depends on $\sigma_1(D)$, etc.

4.2 Bochner Subordination

We start with re-definition of (18), (19). We now define the European Put value with maturity T at the evaluation time $t = X(T_1)$ in the ELVG model

$$P(S_0, T_1 + T, K) = \mathcal{T}_T^S[e^{-rT}P(S_0, T_1, K)]. \quad (35)$$

And, clearly we are interesting in the value of T to be $T = T_2 - T_1$.

Similarly, we define the European Put value with maturity v at the evaluation time $t = T_1$ in the model given by (1) as

$$P^D(S_0, T_1 + v, K) = \mathcal{T}_v^D[e^{-rv}P(S_0, T_1, K)]. \quad (36)$$

By these definitions

$$P(S_0, T_1 + T, K) \Big|_{T=0} = P^D(S_0, T_1 + v, K) \Big|_{v=0} = P(S_0, T_1, K).$$

In contrast to (20), in case of multiple smiles at $t > T_1$ we need to change the definition of t in (16) from $t \mapsto X(t)$ to

$$t \mapsto X(T_1 + t) - X(T_1) \equiv \Delta x(T_1, t). \quad (37)$$

This definition implies two observations.

First, function $\Delta x(T_1, t)$ starts at zero at $t = 0$ and is an increasing function of time. Also, in case $r = q = 0$ we have $\Delta x(T_1, t) = t$. Therefore, $\Delta x(T_1, t)$ can be used as a good clock. Accordingly, similar to (5) we have

$$\mathbb{E}_{\mathbb{Q}}[\Gamma_{\Delta x(T_1, t)}] = \Delta x(T_1, t). \quad (38)$$

Second, a proof that in our model the discounted stock price is a martingale given in Sect. 2 could be repeated for times $t : T_1 < t \leq T_2$. When doing so, at $t > T_1$ we reset the definition of S_t to

$$S_{T_1+t} = D_{\Gamma_{\Delta x(T_1, t)}}, \quad t \geq 0.$$

Then instead of (10) we now have

$$\begin{aligned} \mathbb{E}_{\mathbb{Q}}[dS_{T_1+t}] &= \mathbb{E}_{\mathbb{Q}}[dD_{\Gamma_{\Delta x(T_1, t)}}] = \mu \mathbb{E}_{\mathbb{Q}}[D_{\Gamma_{\Delta x(T_1, t)}} d\Gamma_{\Delta x(T_1, t)}] + \mathbb{E}_{\mathbb{Q}}[\sigma(D_{\Gamma_{\Delta x(T_1, t)}}) dW_{\Gamma_{\Delta x(T_1, t)}}] \\ &= \mu \mathbb{E}_{\mathbb{Q}}[D_{\Gamma_{\Delta x(T_1, t)}}] d\Delta x(T_1, t) = \mu \mathbb{E}_{\mathbb{Q}}[D_{\Gamma_{\Delta x(T_1, t)}}] dX(T_1 + t). \end{aligned} \quad (39)$$

On the other hand,

$$\begin{aligned} \mathbb{E}_{\mathbb{Q}}[d(e^{(q-r)(T_1+t)} S_{T_1+t})] &= e^{(q-r)(T_1+t)} \{ (q-r) \mathbb{E}_{\mathbb{Q}}[S_{T_1+t}] dt + d\mathbb{E}_{\mathbb{Q}}[S_{T_1+t}] \} \\ &= e^{(q-r)t} [\mu + (q-r) S_{T_1} e^{-(r-q)T_1}] dt \end{aligned} \quad (40)$$

One can check, that with $\mu = r - q$ the RHS of (40) vanishes, therefore this construction can be used for option pricing.

The definition in (37) implies that parameter t of the Gamma random clock is reset at the point T_1 , i.e., at $0 \leq t \leq T_1$ it is $t \mapsto X(t) = X(t) - X(0)$, while at $T_1 < t \leq T_2$ it is $t \mapsto X(T_1 + t) - X(T_1)$. Using the definition of $w_i(t)$ in (31), this could be written as

$$t \mapsto \sum_{i=0}^M w_i(T_i + t) [X(T_i + t) - X(T_i)] \quad (41)$$

Resetting t was also first proposed in Carr and Nadtochiy (2017) but in a different form.

Then, the Bochner integral in (16) transforms to

$$\mathcal{T}_T^S P(S, T_1, K) = \int_0^\infty \mathcal{T}_\nu^D P(S, T_1 + \nu, K) \frac{\nu^{m-1} e^{-\nu m / \Delta X(T_1, T)}}{(t^*)^m \Gamma(m)} d\nu. \quad (42)$$

Since for a tractability reason we still want to have $m \equiv \Delta X(T_1, T) / t^* = 1$, we need to redefine t^* in accordance with (41). Based on that, the Bochner integral in (20) now finally reads

$$P(S, T_1 + T, K) = \int_0^\infty P^D(S, T_1 + \nu, K) p e^{-p\nu} d\nu, \quad p \equiv 1 / \Delta X(T_1, T). \quad (43)$$

4.3 Forward Partial Divided-Difference Equation for the Second Term

Now we need to derive a Forward partial divided-difference equation for the second term T_2 similar to how this is done in Sect. 3.2. Obviously, the Put price $P^D(S_0, T_1 + v, K)$ solves the same Dupire equation (26). Therefore, proceeding in the same way as in Sect. 3.2, we apply linear differential operator \mathcal{L} defined in (26) to both parts of (43). Using time-homogeneity of D_t at the interval $[T_1, T_2]$ and again the Dupire equation (26), we obtain

$$\begin{aligned} & -qP(S, T_1 + T, K) - (r - q)K\nabla_K P(S, T_1 + T, K) + \frac{1}{2}\sigma^2(K)\nabla_K^2 P(S, T_1 + T, K) \\ &= \int_0^\infty pe^{-pv} \left[-qP^D(S, T_1 + v, K) - (r - q)K\nabla_K P^D(S, T_1 + v, K) \right. \\ &\quad \left. + \frac{1}{2}\sigma^2(K)\nabla_K^2 P^D(S, T_1 + v, K) \right] dv = \int_0^\infty pe^{-pv} \nabla_v P^D(S, T_1 + v, K) dv \\ &= -pP^D(S, T_1, K) + p \int_0^\infty P^D(S, T_1 + v, K) pe^{-pv} dv \\ &= p[P(S, T_1 + T, K) - P^D(S, T_1, K)] = p[P(S, T_1 + T, K) - P(S, T_1, K)]. \end{aligned} \quad (44)$$

Finally, taking $T = T_2 - T_1$ we obtain an ODE for the Put price $P(S, T_2, K)$.

$$\left[\frac{1}{2}\sigma^2(K)\nabla_K^2 - (r - q)K\nabla_K - \left(q + \frac{1}{X(T_2) - X(T_1)} \right) \right] P(S, T_2, K) = -\frac{P(S, T_1, K)}{X(T_2) - X(T_1)}. \quad (45)$$

Here the local variance function $\sigma^2(K) = \sigma_1^2(K)$ as it corresponds to the interval $[T_1, T_2]$ where the above ODE is solved.

We continue in the same way to derive an ODE for the Put price $P(S, T_i, K)$, $i = 1, \dots, M$, which finally reads

$$\left[\frac{1}{2}\sigma^2(K)\nabla_K^2 - (r - q)K\nabla_K - \left(q + \frac{1}{X(T_i) - X(T_{i-1})} \right) \right] P(S, T_i, K) = -\frac{P(S, T_{i-1}, K)}{X(T_i) - X(T_{i-1})}. \quad (46)$$

This is a recurrent equation that can be solved for all $i = 1, \dots, M$ sequentially starting with $i = 1$ subject to some boundary conditions. The natural boundary conditions for the Put option price are (Hull 1997)

$$\begin{aligned} P(S, T_i, K) &= 0, & K &\rightarrow 0, \\ P(S, T_i, K) &= \mathcal{D}_i K - \mathcal{Q}_i S \approx \mathcal{D}_i K, & K &\rightarrow \infty, \end{aligned} \quad (47)$$

where $\mathcal{D}_i = e^{-rT_i}$ is the discount factor, and $\mathcal{Q}_i = e^{-qT_i}$.

A similar equation can be obtained for the Call option prices, which reads

$$\left[\frac{1}{2}\sigma^2(K)\nabla_K^2 + (r - q)K\nabla_K - \left(q + \frac{1}{X(T_i) - X(T_{i-1})} \right) \right] C(S, T_i, K) = -\frac{C(S, T_{i-1}, K)}{X(T_i) - X(T_{i-1})}, \quad (48)$$

subject to the boundary conditions

$$\begin{aligned} C(S, T_i, K) &= \mathcal{Q}_i S, \quad K \rightarrow 0, \\ C(S, T_i, K) &= 0, \quad K \rightarrow \infty. \end{aligned} \quad (49)$$

5 Solution of the ODE (46)

Below we use the approach similar to Itkin and Lipton (2018) by assuming the local variance to be a piecewise linear continuous function of strike. In contrast to Itkin and Lipton (2018), instead of a standard local volatility model in this paper we use the ELVG model. As the result, instead of a partial differential (Dupire) equation, we face a problem of solving the ODE in (46).

First, it is useful to change the dependent variable from $P(S, T_j, K)$ to

$$V(S, T_j, K) = P(S, T_j, K) - \mathcal{D}_j K,$$

which is known as a *covered Put*. The advantage of the covered Put is that according to (47) its price obeys homogeneous boundary conditions.

Using this definition we now re-write (46) in a more convenient form (while with some loose of notation)

$$\begin{aligned} -v(x)V_{xx}(x) + b_1 x V_x(x) + b_{0j} V(x) &= c_j, \\ b_1 &= (r - q)p_j, \quad b_{0j} = qp_j + 1, \quad c_j = V(T_{j-1}, x) + \beta x, \\ p_j &= X(T_j) - X(T_{j-1}) > 0, \quad x = \frac{K}{S}, \quad V(x) = V(S, T_j, x), \quad v(x) = p_j \frac{\sigma^2(x)}{2S^2}, \\ \beta &= -S[\mathcal{D}_j(1 + p_j r) - \mathcal{D}_{j-1}]. \end{aligned} \quad (50)$$

In (50) x is the inverse moneyness. In what follows we also assume that $r > q > 0$, but this assumption could be easily relaxed.

Further, suppose that for each maturity T_j , $j \in [1, M]$ the market quotes are provided at a set of strikes K_i , $i = 1, \dots, n_j$ where the strikes are assumed to be sorted in the increasing order. Then the corresponding continuous piecewise linear local variance function $v_j(x)$ on the interval $[x_i, x_{i+1}]$ reads

$$v_{j,i}(x) = v_{j,i}^0 + v_{j,i}^1 x, \quad (51)$$

where we use the super-index 0 to denote a level v^0 , and the super-index 1 to denote a slope v^1 . Subindex $i = 0$ in $v_{j,0}^0, v_{j,0}^1$ corresponds to the interval $(0, x_1]$. Since $v_j(x)$ is continuous, we have

$$v_{j,i}^0 + v_{j,i}^1 x_{i+1} = v_{j,i+1}^0 + v_{j,i+1}^1 x_{i+1}, \quad i = 0, \dots, n_j - 1. \quad (52)$$

The first derivative of $v_j(x)$ experiences a jump at points x_i , $i \in \mathbb{Z} \cap [1, n_j]$. We also assume that $v(x, T)$ is a piecewise constant function of time, i.e., $v_{j,i}^0, v_{j,i}^1$ don't depend on T on the intervals $[T_j, T_{j+1})$, $j \in [0, M - 1]$, and jump to new values at the points T_j , $j \in \mathbb{Z} \cap [1, M]$.

With the above assumptions in mind, (50) can be solved by induction. One starts with $T_0 = 0$, and on each time interval $[T_{j-1}, T_j]$, $j \in \mathbb{Z} \cap [1, M]$ solves the problem (50) for $V(x) \mapsto P(S, T_j, x) - d_j Sx$.

Since $v(x)$ is a piecewise linear function, the solution of (50) can also be constructed separately for each interval $[x_{i-1}, x_i]$. By taking into account the explicit representation of $v(x)$ in (51), from (50) for the i -th spatial interval we obtain

$$\begin{aligned} & -(b_2 + a_2x)V_{xx}(x) + b_1xV_x(x) + b_0V(x) = c \\ & b_2 = v_{j,i}^0, \quad a_2 = v_{j,i}^1. \end{aligned} \quad (53)$$

We proceed by introducing a new independent variable $z = (b_2 + a_2x)b_1/a_2^2$, $z \in \mathbb{R}^+$, so that (53) transforms to

$$\begin{aligned} & -zV_{zz}(z) + (z - q_2)V_z(z) + q_1V(z) = \chi \\ & q_1 = b_0/b_1, \quad q_2 = b_2b_1/a_2^2, \quad \chi = c/b_1. \end{aligned} \quad (54)$$

The (54) is an *inhomogeneous* Laplace equation (Polyanin and Zaitsev 2003, page 155). It is well known that if $y_1 = y_1(z)$, $y_2 = y_2(z)$ are two fundamental solutions of the corresponding *homogeneous* equation, then the general solution of (54) can be represented as

$$\begin{aligned} V(z) &= C_1y_1(z) + C_2y_2(z) + \frac{1}{b_1}I_{12}(z) \\ I_{12}(z) &= -y_2(z) \int \frac{y_1(z)f(z)}{W_z} dz + y_1(z) \int \frac{y_2(z)f(z)}{W_z} dz \equiv I_1 + I_2, \\ f(z) &= V(T_{j-1}, z) - k_1 - k_2z, \quad k_1 = \beta \frac{b_2}{a_2}, \quad k_2 = -\beta \frac{a_2}{b_1}, \end{aligned} \quad (55)$$

where $W = y_1(y_2)_z - y_2(y_1)_z$ is the so-called Wronskian, and β is defined in (50). Then the problem is to determine suitable fundamental solutions of the homogeneous Laplace equations. Based on Polyanin and Zaitsev (2003), if $a_2 \neq 0$, they read

$$y_i(z) = \mathcal{V}_i(q_1, q_2, z), \quad i = 1, 2 \quad (56)$$

Here $\mathcal{V}_i(a, b, z)$ is an arbitrary solution of the degenerate hypergeometric equation, i.e., Kummer's function (Abramowitz and Stegun 1964). Two types of Kummer's functions are known, namely $M(a, b, z)$ and $U(a, b, z)$, which are Kummer's functions of the first and second kind.

It is known, that there exist several pairs of such independent solutions. Therefore, for every spatial interval in z among all possible fundamental pairs we have to determine just one which is numerically satisfactory at this interval (see Olver (1997) for the detailed definition of satisfactory solutions and the corresponding discussion). Since our boundary conditions are set at zero and positive infinity, we need a numerically satisfactory solution for the positive half of the real line.

Similar to Itkin and Lipton (2018), in the vicinity of the origin we choose the numerically satisfactory pair as (Olver 1997),

$$\begin{aligned}
y_1(\chi) &= M(q_1, q_2, z) = e^z M(q_2 - q_1, q_2, -z), \\
y_2(\chi) &= z^{1-q_2} M(q_1 - q_2 + 1, 2 - q_2, z) = z^{1-q_2} e^z M(1 - q_1, 2 - q_2, -z), \\
W &= \sin(\pi q_2) z^{-q_2} e^z / \pi.
\end{aligned} \quad (57)$$

However, in the vicinity of infinity the numerically satisfactory pair is (Olver 1997)

$$\begin{aligned}
y_1(\chi) &= U(q_1, q_2, z) = z^{1-q_2} U(q_1 - q_2 + 1, 2 - q_2, z), \\
y_2(\chi) &= e^z U(q_2 - q_1, q_2, -z) = e^z z^{1-q_2} U(1 - q_1, 2 - q_2, -z), \\
W &= (-1)^{q_1-q_2} e^z z^{-q_2}.
\end{aligned} \quad (58)$$

As two solutions $J_1(q_1, q_2, z), J_2(q_1, q_2, z)$ are independent, (55) is a general solution of (54). Two constants C_1, C_2 should be determined based on the boundary conditions for the function $V(z)$.

The boundary conditions for the ODE (53) in a strike K space (or in x space) should be set at zero and infinity. Based on the usual shape of the local variance curve and its positivity, for $x \rightarrow 0$, we expect that $v_{j,i}^1 < 0$. Similarly, for $x \rightarrow \infty$ we expect that $v_{j,i}^1 > 0$. In between these two limits the local variance curve for a given maturity T_j is assumed to be continuous, but the slope of the curve could be both positive and negative, see, e.g., Itkin (2015) and references therein. Also, by definition $z = v_{j,i}$, and $\text{Dom}(z) = \mathbb{R}^+$. Thus, at high strikes $a_2 = v_{j,i}^1 > 0$. Therefore, the boundary conditions for (54) should be set at $z = b_2$ (which corresponds to the boundary $K = 0$) and at $z \rightarrow \infty$. These are the boundary conditions given in (47).

6 Computation of the Source Term

Computation of the source term pI_{12} in (55) could be achieved in several ways. The most straightforward one is to use numerical integration as the Put price $P(x, T_{i-1})$ as a function of x is already known when we solve (50) for $T = T_i$. However, as this is discussed in detail in Itkin and Lipton (2018), function $P(x, T_{i-1})$ is known only for a discrete set of points in x . Therefore, some kind of interpolation is necessary to find its values at the other points.

6.1 No-Arbitrage Interpolation

As shown in Itkin and Lipton (2018), this interpolation must preserve no-arbitrage. So, for instance, a standard linear interpolation is not a good candidate, since it violates no-arbitrage conditions. Indeed, given three Put option prices $P(K_1), P(K_2), P(K_3)$ for three strikes $K_1 < K_2 < K_3$, the necessary and sufficient conditions for an arbitrage-free system read (Cox and Rubinstein 1985),

$$\begin{aligned}
P(K_3) &> 0, \quad P(K_2) < P(K_3), \\
Bs &= (K_3 - K_2)P(K_1) - (K_3 - K_1)P(K_2) + (K_2 - K_1)P(K_3) > 0.
\end{aligned} \quad (59)$$

Suppose that we want to use linear interpolation in the strike space on the interval $[K_1, K_3]$ to find the unknown Put option price $P(K_2)$ given the values of $P(K_1), P(K_3)$,

$$P(K_2) \equiv P_l(K_2) = \frac{P(K_1)K_3 - P(K_3)K_1}{K_3 - K_1} + \frac{P(K_3) - P(K_1)}{K_3 - K_1}K_2.$$

When plugging this expression into the second line of (59), the left hands side of the latter vanishes, so the third no-arbitrage condition is violated.

In Itkin and Lipton (2018) it is shown that this problem could be resolved if we use linear interpolation with a modified independent variable (further on we denote it as $P_F(K)$),

$$\begin{aligned} P(K_2) &\equiv P_F(K_2) \\ &= \frac{P(K_1)f(K_3) - P(K_3)f(K_1)}{f(K_3) - f(K_1)} + \frac{P(K_3) - P(K_1)}{f(K_3) - f(K_1)}f(K_2), \end{aligned} \quad (60)$$

where $f(K)$ is a convex and increasing function in $[K_1, K_3]$. Indeed, if $f(K)$ is convex, then $P(K_2) = P_F(K_2) = P_l(K_2) - \varepsilon$, $\varepsilon > 0$ (see Fig. 2 in Itkin and Lipton (2018)). Substitution of this expression into the second line of (59) gives $(K_3 - K_1)\varepsilon > 0$, which is true. The second condition in (59) now reads

$$(P(K_1) - P(K_3))(f(K_3) - f(K_2))(f(K_1) - f(K_3)) > 0,$$

which is also true since $f(K)$ is an increasing function of K .

Alternatively, one can use non-linear interpolation. In Itkin and Lipton (2018)) both approaches were combined, and it was proved that the new interpolation scheme preserves no-arbitrage. Moreover, the final representation of the modified Put price (which is a dependent variable in their approach) obtains a nice tractable representation, so the integral I_{12} can be computed in closed form. Here we want to exploit the same idea, thus significantly improving performance of our model as compared with the numerical integration.

Therefore, here we propose the following interpolation scheme

$$\begin{aligned} P(x) &\equiv P_F(x) = \gamma_1 + \gamma_2 x^2, \quad x_1 \leq x \leq x_3, \\ \gamma_1 &= \frac{P(x_3)x_1^2 - P(x_1)x_3^2}{x_1^2 - x_3^2}, \quad \gamma_2 = \frac{P(x_1) - P(x_3)}{x_1^2 - x_3^2}. \end{aligned} \quad (61)$$

Then Proposition similar to that in Itkin and Lipton (2018) can be proved.

Proposition 1 *The interpolation scheme in (61) is arbitrage free at the interval $[K_1, K_3]$.*

Proof Observe, that the no-arbitrage conditions in (59) are discrete versions of the conditions

$$P > 0, \quad P_K > 0, \quad P_{K,K} > 0,$$

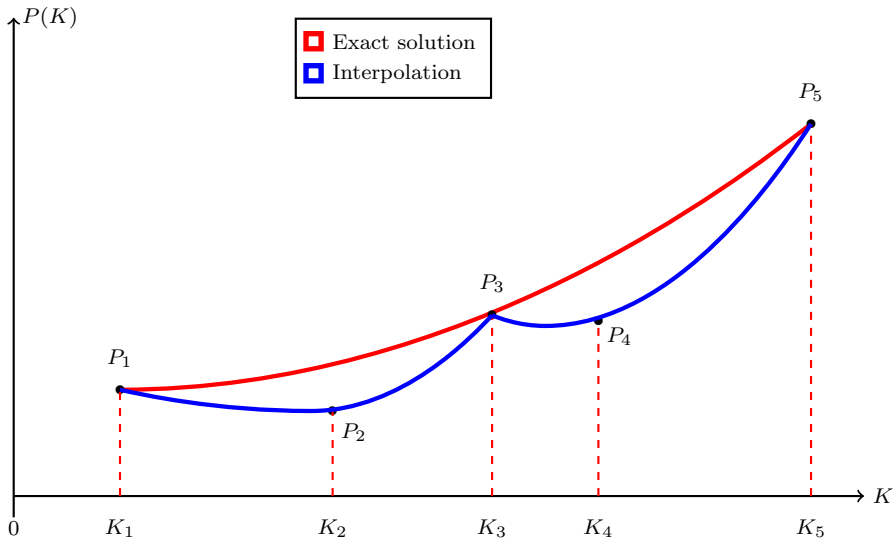


Fig. 1 Three strikes K_2, K_3, K_4 which belong to the consecutive intervals

They, in turn, correspond to the conditions

$$P > 0, \quad P_x > 0, \quad P_{x,x} > 0,$$

as $x'(K) = 1/S > 0$. By differentiating the first line of (61) one can check that the proposed interpolation obeys these conditions provided that P is an increasing function of K (or x) given the values of all other parameters to be constant. For instance, this is the case for the Black–Scholes Puts. \square

As by definition z is a linear function of x , a similar interpolation scheme can be used in the z space, with a similar proof of no-arbitrage.

6.2 No-Arbitrage at Consecutive Intervals

Proposition 1 guarantees that the proposed interpolation doesn't introduce an arbitrage into the solution if any three strikes belong to the same interval $[K_1, K_3]$. However, what if we consider strikes K_2, K_3, K_4 as this is schematically depicted in Fig. 1.

Here at the interval $[K_1, K_3]$ the exact solution is depicted by the red line, while our quadratic interpolation is in blue. Accordingly, the Put prices P_1, P_3 are the market quotes, so they assumed to be the exact prices with no market arbitrage. By our construction, these prices also don't have a model arbitrage. At the consecutive interval $[K_3, K_5]$ a similar construction applies.

We have to emphasize that this graph is pure illustrative, and no-arbitrage interpolation guarantees that $P'(K) > 0$, while the blue line in Fig. 1 doesn't support this. However, if we draw an accurate picture by using the above formulae, it would be

Table 1 Parameters of the test for non-negativity of the Butterfly spread. σ_{BS} is the Black–Scholes implied volatility

Test	S	r	σ_{BS}	T	K_1	K_3	K_5
1	100	0.01	0.5	2	80	100	130
2	100	0.1	0.1	0.1	90	100	105

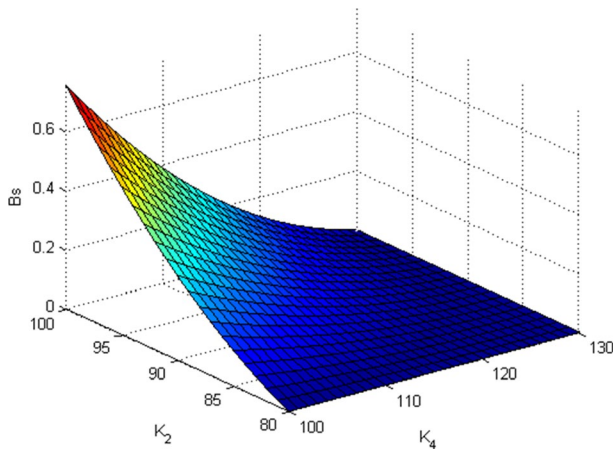


Fig. 2 Butterfly spread B_s for a set of strikes K_2, K_3, K_4 computed in Test 1 in Table 1

almost impossible to distinguish the red and blue lines. Therefore, we changed convexity and skew of the blue line to make the difference visible.

By Proposition 1 given a set of strikes K_1, K_2, K_3 the price P_2 obtained by interpolation preserves no-arbitrage. The same is true for P_5 given the Put prices P_3, P_5 at strikes K_3, K_5 . Now assume that given K_1, K_3, K_5 and P_1, P_3, P_5 we want to check the no-arbitrage conditions for the set of strikes K_2, K_3, K_4 . The Proposition 1 doesn't help in this situation, so we need a special consideration of this case.

Obviously, the first and second conditions in (59) are still satisfied in this case, so we need to check that the butterfly spread is positive. Unfortunately, at the moment we don't have a general analytical solution of this problem, while some particular cases can be addressed. Thus this remains an open question. However, we checked this condition numerically. In doing so we used the Black–Scholes Put prices P_1, P_3, P_5 ⁴ and built a 2D plot of B_s which is the left-hand side of the third line in (59). The results for two cases presented in Table 1 are presented in Figs. 2 and 3.

Overall, we ran a lot of tests and didn't find any case where the butterfly spread would become negative. This partly supports our no-arbitrage interpolation. More sophisticated cases where, e.g., instead of strike K_3 in the butterfly spread at strikes K_2, K_3, K_4 we use another strike K_6 such that $K_1 < K_2 < K_3 < K_4 < K_6 < K_5$, could be treated in a similar way. Again, our numerical tests didn't reveal any case where a butterfly spread would become negative.

⁴ This is done to preserve upper bounds on the Put price that $P(S, K, T, r) \leq Ke^{-rT}$ (Levy 1985).

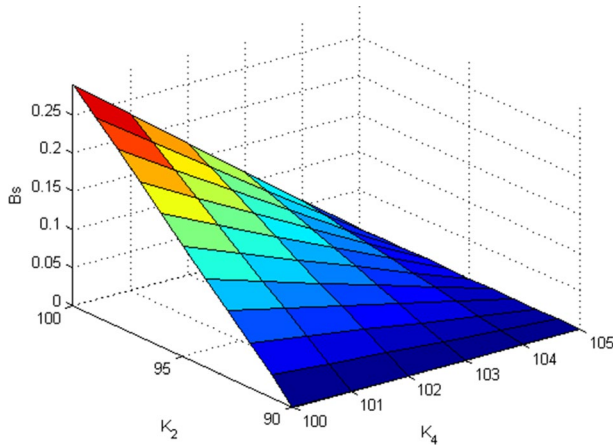


Fig. 3 Butterfly spread B_s for a set of strikes K_2, K_3, K_4 computed in Test 2 in Table 1

6.3 Computing the Integrals in (55) Far from $z = 0$

Using the interpolation scheme proposed in above, consider the first integral in (55). To remind, we compute it at some interval $z \in [z_i, z_{i+1}]$, $i \in \mathbb{Z} \cap [1, n_j]$. Picking together the solutions in (57) with the interpolation scheme for $P(z, T_{j-1})$ and Wronskians in (57), and substituting them into the first integral in (55) we obtain

$$\begin{aligned}
 \int \frac{y_2(z)f(z, T_{j-1})}{Wz} dz &= A \left[-B_0 + B_1 M(-2 - q_1, -1 - q_2, -z) + B_2 M(-1 - q_1, -q_2, -z) \right. \\
 &\quad \left. + B_3 M(-q_1, 1 - q_2, -z) \right], \\
 A &= \frac{1}{b_1^2 q_1} \pi (1 - q_2) \csc(\pi q_2), \\
 B_0 &= \frac{1}{a_2^2 (q_1 + 1)(q_1 + 2)} \left[a_2 b_1 (q_1 + 2) (a_2^2 \beta q_2 - b_1 (q_1 + 1) (\beta b_2 - a_2 \gamma_1)) \right. \\
 &\quad \left. + \gamma_2 (2a_2^4 q_2 (q_2 + 1) - 2a_2^2 b_1 b_2 (q_1 + 2) q_2 + b_1^2 b_2^2 (q_1 + 1)(q_1 + 2)) \right], \\
 B_1 &= 2a_2^2 \gamma_2 \frac{q_2 (q_2 + 1)}{(1 + q_1)(2 + q_1)}, \\
 B_2 &= (a_2 b_1 \beta - 2b_1 b_2 \gamma_2 + 2a_2^2 \gamma_2 z) \frac{q_2}{1 + q_1}, \\
 B_3 &= \frac{1}{a_2^2} \left[a_2 b_1 (a_2^2 \beta z + a_2 b_1 \gamma_1 - \beta b_1 b_2) + \gamma_2 (b_1 b_2 - a_2^2 z)^2 \right].
 \end{aligned} \tag{62}$$

Similarly

$$\begin{aligned}
\int \frac{y_1(z)f(z, T_{j-1})}{Wz} dz &= \bar{A} \left[\bar{B}_1 M(q_2 - q_1, 1 + q_2, -z) + \bar{B}_2 {}_2F_2(q_2 - q_1, 1 + q_2; q_2, 2 + q_2; -z) \right. \\
&\quad \left. + \bar{B}_3 {}_2F_2(q_2 - q_1, 2 + q_2; q_2, 3 + q_2; -z) \right], \\
A &= \pi z^{q_2} \csc(\pi q_2) \Gamma(q_2), \\
B_1 &= \frac{a_2^2 \gamma_1 - a_2 \beta b_2 + b_2^2 \gamma_2}{a_2^2 \Gamma(1 + q_2)}, \\
B_2 &= \frac{\Gamma(q_2 + 1)}{\Gamma(q_2) \Gamma(2 + q_2) b_1} (a_2 \beta - 2b_2 \gamma_2) z, \\
B_3 &= \frac{\Gamma(q_2 + 1)}{\Gamma(q_2) \Gamma(3 + q_2) b_1^2} a_2^2 (1 + q_2) \gamma_2 z^2,
\end{aligned} \tag{63}$$

where ${}_pF_q(a_1, \dots, a_p; b_1, \dots, b_q; z)$ is the generalized hypergeometric function (Olver 1997).

6.4 Computing the Integrals in (55) Far from $z = \pm\infty$

Here we proceed in the same way as in the previous section. Again, we pick together the solutions in (58) with the interpolation scheme for $P(z, T_{j-1})$ and Wronskians in (58), and substitute them into the first integral in (55) we obtain

$$\begin{aligned}
\int \frac{y_2(z)f(z, T_{j-1})}{Wz} dz &= (-1)^{q_2 - q_1} [C_0 J_0 + C_1 J_1 + C_2 J_2], \\
J_i &= \int z^i U(1 - q_1, 2 - q_2, -z) dz, \\
C_0 &= \frac{b_2^2 \gamma_2}{a_2^2} - \frac{\beta b_2}{a_2} + \gamma_1, \quad C_1 = \frac{a_2 \beta - 2b_2 \gamma_2}{b_1}, \quad C_2 = \frac{a_2^2 \gamma_2}{b_1^2}.
\end{aligned} \tag{64}$$

It is known (Abramowitz and Stegun 1964), that

$$J_0 = -\frac{1}{q_1} U(-q_1, 1 - q_2, -z).$$

Then, J_1, J_2 can be found using integration by parts to yield

$$\begin{aligned}
J_1 &= z J_0 + \frac{1}{q_1(1 + q_1)} U(-1 - q_1, -q_2, -z), \\
J_2 &= z J_1 + \frac{1}{q_1(2 + 3q_1 + q_1^2)} U(-2 - q_1, -1 - q_2, -z) - z \frac{1}{q_1(1 + q_1)} U(-1 - q_1, -q_2, -z).
\end{aligned}$$

Similarly

$$\int \frac{y_1(z)f(z, T_{j-1})}{Wz} dz = (-1)^{q_2-q_1} [C_0 \mathcal{J}_0 + C_1 \mathcal{J}_1 + C_2 \mathcal{J}_2], \quad (65)$$

$$\mathcal{J}_i = \int z^i e^{-z} U(1 + q_1 - q_2, 2 - q_2, z) dz.$$

The integrals \mathcal{J}_i have been considered in Itkin and Lipton (2018) using the approach of Ng and Geller (1970). Borrowing from there the result

$$\mathcal{J}_0 = \int e^{-z} U(1 + q_1 - q_2, 2 - q_2, z) dz = -e^{-z} U(q_1 - q_2, 1 - q_2, z),$$

and using integration by parts, we obtain

$$\begin{aligned} \mathcal{J}_1 &= z \mathcal{J}_0 + e^{-z} U(q_1 - q_2 - 1, -1 - q_2, z), \\ \mathcal{J}_2 &= z \mathcal{J}_1 - \int \mathcal{J}_1 dz = (z - 1) \mathcal{J}_1 - \int e^{-z} U(q_1 - q_2 - 1, -1 - q_2, z) dz \\ &= (z - 1) \mathcal{J}_1 + e^{-z} U(q_1 - q_2 - 2, -2 - q_2, z). \end{aligned}$$

7 Calibration of Smile for a Given Term T_i

Calibration problem for the local volatility model can be formulated as follows: given market quotes of Call and/or Put options corresponding to a set of N strikes $\{K\} := K_j, j \in [1, N]$ and same maturity T_i , find the local variance function $\sigma(K)$ such that these quotes solve equations in (46), (48).

As mentioned in Itkin and Lipton (2018), there are two main approaches to solving this problem. The first approach attempts to construct a continuous implied volatility (IV) surface matching the market quotes by using either some parametric or non-parametric regression, and then generates the corresponding LV surface via the well-known relationship between the local and implied variances also known as the Dupire formula, see, e.g., Itkin (2015) and references therein. To be practically useful, this construction should guarantee no arbitrage for all strikes and maturities, which is a serious challenge for any model based on interpolation. If the no-arbitrage condition is satisfied, then the LV surface can be calculated using the Dupire formula. The second approach relies on the direct solution of the corresponding forward equation (which is the Dupire equation in the Black–Scholes world, or (48), (46) in our model) using either analytical or numerical methods. The advantage of this approach is that it guarantees no-arbitrage. However, the problem of the direct solution can be ill-posed (Coleman et al. 2001), and is rather computationally intensive.

In this section we show that the second approach could be significantly simplified when using the ELVG model, so calibration of the smile could be done very fast and accurate.

Further, for the sake of certainty, suppose that all known market quotes are Puts, despite this can be easily relaxed. Also, suppose that the shape of a local variance

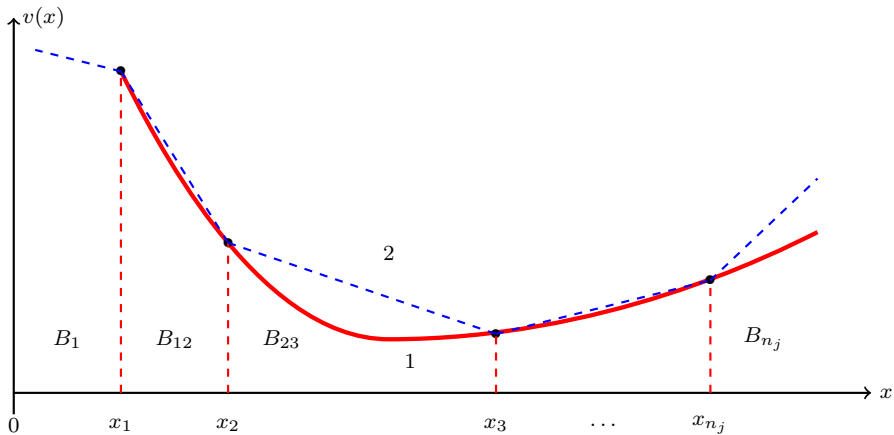


Fig. 4 Construction of the combined solution in $x \in \mathbb{R}^+$: 1 (red solid line—the real (unknown) local variance curve, 2 (dashed blue line)—a piecewise linear solution

is given by some function $\sigma_j(K) = f_j(K, p_1, \dots, p_L)$, where p_1, \dots, p_L is a set of the model parameters to be determined. For instance, in Lipton and Sepp (2011); Carr and Nadtochiy (2017) the local variance is assumed to be a piecewise constant function of strike, while in Itkin and Lipton (2018) this is a piecewise linear function of strike.

In this paper we also assume the local variance to be a piecewise linear function of strike. Moreover, for our model we obtained a closed form representation of the Put option prices via parameters of the model given in Sects. 5, 6. Therefore, calibration of the model to the given set of smiles could be provided as follows. First, using the above-mentioned closed form solution for a fixed interval in x where parameters of the model are constant, we construct the combined solution valid for all $x \in \mathbb{R}^+$. At the second step, the parameters of the local variance function $v_{j,i}^0, v_{j,i}^1$ can be found together with the integration constants C_1, C_2 in (55) by solving a system of non-linear algebraic equations.

7.1 The Combined Solution in $x \in \mathbb{R}^+$

Suppose that the Put prices for $T = T_j$ are known for n_j ordered strikes. The location of these strikes on the x line is schematically depicted in Fig. 4.

Recall, that the Put prices are given by (55), which in a more convenient form at the interval $x_{i-1} \leq x \leq x_i$ and at $T = T_j$ can be represented as

$$P_i(x) = C_{j,i}^{(1)} \mathcal{J}_1(q_1, q_2, z) + C_{j,i}^{(2)} \mathcal{J}_2(q_1, q_2, z) + \frac{1}{b_1} I_{12}(z) + \mathcal{D}_j K, \quad (66)$$

$$z \equiv (b_2 + a_2 x) b_1 / a_2^2 = (v_{j,i}^0 + v_{j,i}^1 x) b_1 / a_2^2.$$

Here, for consistency we change notation of two integration constants which belong to the i -th interval in x and j -th maturity to $C_{j,i}^{(1)}, C_{j,i}^{(2)}$.

For the open interval B_1 in Fig. 4, since function $K_v(z)$ diverges when $z \rightarrow 0$, we have to put $C_{j,1}^{(1)} = 0$ as the boundary condition⁵. Therefore, (66) contains just one yet unknown constant $C_{j,1}^{(2)}$. For the closed intervals $x \in [x_{i-1}, x_i]$, $i \in [2, n_j]$ the solutions in (66) have two yet unknown constants $C_{j,i}^{(1)}$, $C_{j,i}^{(2)}$, since x is finite on the corresponding intervals, and both solutions $y_1(x), y_2(x)$ are well-behaved. Finally, for the interval $x \in [x_{n_j}, \infty)$, according to the boundary conditions in (47) we must set $C_{2,n_j+1}^{(2)} = 0$.

Rigorously speaking, we also have to show that in the limits $x \rightarrow 0$ and $x \rightarrow \infty$ the source term $I_{12}(z)$ in (55) also vanishes. This could be done similar to Proposition 2 in Itkin and Lipton (2018).

Thus, we have $2n_j$ unknown constants to be determined. Since the local volatility function v_i is continuous at the points x_i , $i = 1, \dots, n_j$, so should be the Put options prices $P(x, T_j)$. Therefore, we require that at the points x_i , $i = 1, \dots, n_j$ the solution for Puts and its first derivative in x should be a continuous function of x . Thus, if the local variance function is known, the above constants solve a system of $2n_j$ algebraic equations. This system has a block-diagonal structure where each block is a 2×2 matrix. Therefore, it can be easily solved with the linear complexity $O(n_j)$.

When computing the first derivatives, we take into account that (Abramowitz and Stegun 1964),

$$\begin{aligned} \frac{\partial M(a, b, z)}{\partial z} &= \frac{a}{b} M(a+1, b+1, z), \quad \frac{\partial U(a, b, z)}{\partial z} = -aU(a+1, b+1, z), \\ \partial_z I_{12}(z) &= \left[\frac{y_1'(z)}{y_1(z)} I_1 + \frac{y_2'(z)}{y_2(z)} I_2 \right] a_2. \end{aligned} \quad (67)$$

Therefore, computing the derivatives of the solution doesn't cause any new technical problem.

7.2 Additional Equations for Calibration

As we have already mentioned above, the standard way of doing calibration of the local volatility model would be that described, e.g., in Itkin and Lipton (2018). Namely, given the maturity T_j and some initial guess of the local variance parameters $v_{j,i}^0, v_{j,i}^1, \forall i \in [1, n_j]$, the following steps represented in Panel 1 have to be achieved, e.g., in the standard least-square method,

⁵ Actually, since $x \rightarrow 0$ implies $z = v \rightarrow b_2$, so b_2 should be non-negative, $b_2 \geq 0$. Therefore, the only case when $z \rightarrow 0$ at $x \rightarrow 0$ is when $b_2 = 0$.

Input: Strikes z_i , $i \in [1, n_j]$, Put prices V_i^{market} , $i \in [1, n_j]$
Output: $v_{j,i}^0, v_{j,i}^1, \forall i \in [1, n_j]$
Initialization: The initial guess of $v_{j,i}^0, v_{j,i}^1, \forall i \in [1, n_j]$, the tolerance ϵ ;
while 1 **do**
 1. Solve the system for $C_{j,i}^{(1)}, C_{j,i}^{(2)}$;
 2. Compute Put option prices $V(x)$;
 3. Compute the total error $\Delta = \sum_{i=1}^{n_j} [V(x_i) - V^{market}(x_i)]^2$;
 if $\Delta > \epsilon$ **then**
 New guess for $v_{j,i}^0, v_{j,i}^1, \forall i \in [1, n_j]$;
 else
 break;
 end
end

Here $V^{market}(z_i)$ are the market Put quotes at the given strikes and maturity. Obviously, when the number of calibration parameters (strikes) is high, this algorithm is slow even if the closed form solution is known and can be used at Step 2. Things become even worse when a numerical solution at Step 2 has to be used if the closed form solution is not available.

However, in our case this tedious algorithm can be fully eliminated. Indeed, at every point i in strike space, $i \in [1, n_j]$ we have four unknown variables $v_{j,i}^0, v_{j,i}^1, C_{j,i}^{(1)}, C_{j,i}^{(2)}$. We also have four equations which contain these variables, namely

$$\begin{aligned} P_i(x)|_{x=x_i} &= P_{i+1}(x)|_{x=x_i}, \\ P_i(x)|_{x=x_i} &= P_{market}(x_i), \\ \frac{\partial P_{i+1}(x)}{\partial x} \Big|_{x=x_i} &= \frac{\partial P_i(x)}{\partial x} \Big|_{x=x_i}, \\ v_{j,i}^0 + v_{j,i}^1 x_i &= v_{j,i+1}^0 + v_{j,i+1}^1 x_i, \quad i = 1, \dots, n_j. \end{aligned} \quad (68)$$

Also, based on (52), the last line in (68) could be re-written as a recurrent expression

$$v_{j,i}^0 = v_{j,n_j}^0 + \sum_{k=i+1}^{n_j} x_k (v_{j,k}^1 - v_{j,k-1}^1), \quad i = 0, \dots, n_j - 1. \quad (69)$$

The (68) is a system of $4n_j$ nonlinear equations with respect to $4(n_j + 1)$ variables $v_{j,i}^0, v_{j,i}^1, C_{j,i}^{(1)}, C_{j,i}^{(2)}$. We remind that according to the boundary conditions $C_{j,1}^{(1)} = C_{j,n_j}^{(2)} = 0$. Therefore, we need two additional conditions to provide a unique solution. For instance, often traders have an intuition about the asymptotic behavior of the volatility surface at infinity, which, according to our construction, is determined by v_{j,n_j}^1 and $v_{j,0}^1$.

Overall, solving the nonlinear system of equations (68) provides the final solution of our problem. This can be done by using standard methods, and, thus, no any optimization procedure is necessary. However, a good initial guess still would be helpful for a better (and faster) convergence.

7.3 Smart Initial Guess

The initial guess of the solution of (66) can be constructed, for instance, as follows. We take advantage of the fact that according to (50) the local variance function $v(x)$ could be explicitly expressed as

$$v(x) = \frac{b_1 x V_x(x) + b_0 V(x) - c}{V_{x,x}(x)}. \quad (70)$$

Given maturity T_j and approximating derivatives by central finite differences with the second order of approximation in step h in the strike space (see, e.g. Itkin 2017), (70) can be represented in the form

$$\begin{aligned} v_{j,i}^0 + v_{j,i}^1 x_i &= \frac{b_1 x V_x(x_i) + b_{0,j} V(x_i) - c_j}{V_{x,x}(x_i)}, \\ V_x(x_i) &= \alpha_{-1} V(x_{i-1}) + \alpha_0 V(x_i) + \alpha_1 V(x_{i+1}), \\ V_{x,x}(x_i) &= \delta_{-1} V(x_{i-1}) + \delta_0 V(x_i) + \delta_1 V(x_{i+1}), \\ \alpha_{-1} &= -\frac{h_{i+1}}{h_i(h_{i+1} + h_i)}, \quad \alpha_0 = \frac{h_{i+1} - h_i}{h_{i+1} h_i}, \quad \alpha_1 = \frac{h_i}{h_{i+1}(h_{i+1} + h_i)}, \\ \delta_{-1} &= \frac{2}{h_i(h_{i+1} + h_i)}, \quad \delta_0 = -\frac{2}{h_{i+1} h_i}, \quad \delta_1 = \frac{2}{h_{i+1}(h_{i+1} + h_i)}, \\ h_i &= x_i - x_{i-1}, \quad i \in [1, n_j]. \end{aligned} \quad (71)$$

Further, associating Put prices $P(S, T_j, x_i)$ with the given market quotes, the right hands side of the first line in (71) can be found explicitly. This then can be combined with the last line of (68) to produce a system of $2(n_j - 1)$ equations for $v_{j,i}^1$ and $v_{j,i}^1$, $i \in [1, n_j]$. Finally, we take into account the asymptotic behavior of the volatility surface in x at zero and infinity, which, according to our construction, is determined by v_{j,n_j}^1 and $v_{j,0}^1$ and is assumed to be known. Thus, we obtain a closed system of $2(n_j - 1)$ linear equations with a banded matrix which can be easily solved with a linear complexity. This provides an explicit representation of the local variance function over the whole set of intervals in the strike space determined according to our approximation where the continuous derivatives are replaced by finite differences.

Note, that at the first and last strike intervals the approximation of the first and second derivatives by central finite differences should be replaced by one-sided approximations, in more detail see Itkin (2017), chapter 2.

It could also happen that at some strikes this solution (the smart guess) gives rise to a negative local variance. In such a case we do another step which is a kind of smoothing. Namely, we exclude from the initial guess all values where the local variance is negative and using the remaining points create a spline. Then the negative values in the initial guess are replaced by those given by the constructed spline.

The final step utilizes the exact representation (66) of the Put price in the ELVG model. As the variance function is already known from the previous step, this equation contains two yet unknown constants $C_{j,i}^{(1)}, C_{j,i}^{(2)}$. Accordingly, they can be found by solving the system of 2 linear equations represented by the first and third lines of (68). Then, after this last step is complete, all unknown variables are determined, and thus found solution could be used as an educated initial guess for solving (68) numerically.

8 Asymptotic Solutions

In many practical situations either some coefficients $a_2 = v_{j,i}^1$, or both $b_2 = v_{j,i}^0$, $a_2 = v_{j,i}^1$ in (53) are small. Of course, in that case the general solution (66) remains valid. However, in this case when computing the values of Kummer functions numerically, numerical errors significantly grow. This is especially pronounced when computing the integral I_{12} . The main point is that either the Kummer function takes a very small value, and then the constants $C_{j,i}^{(1)}, C_{j,i}^{(2)}$ should be big to compensate, or vice versa. Resolution of this requires a high-precision arithmetics, and, which is more important, taking many terms in a series representation of the Kummer functions, which significantly slows down the total performance of the method.

On the other hand, to eliminate these problems we can look for asymptotic solutions of (53) taking into account the existence of small parameters from the very beginning. This approach was successfully elaborated on in Itkin and Lipton (2018), and below we proceed in a similar spirit.

8.1 Small a_2

We can build the solution of (54) directly using an independent variable x (so not switching to the variable z). We represent it as a series on the small parameter a_2 , i.e.

$$V(x) = \sum_{i=0}^{\infty} a_2^i V_i(x). \quad (72)$$

In the zero-order approximation by plugging (72) into (54) and neglecting by terms proportional to $a_2 \ll 1$ we obtain the following equation for $V_0(x)$

$$-b_2 V_{xx}(x) + b_1 x V_x(x) + b_0 V(x) = c. \quad (73)$$

This equation is simpler than (66). Still, its solution is given by a general formula

$$V(x) = C_1 y_1(x) + C_2 y_2(x) + I_{12}(x),$$

but the fundamental solutions $y_1(x), y_2(x)$ now read

$$y_1(x) = \mathcal{H}\left(-\frac{b_0}{b_1}, \sqrt{\frac{b_1}{2b_2}}x\right), \quad y_2(x) = M\left(\frac{b_0}{2b_1}, \frac{1}{2}, \frac{b_1}{2b_2}x^2\right),$$

where $\mathcal{H}(a, x)$, $a, x \in \mathbb{R}$ is the generalized Hermite polynomial $H_a(x)$ (Abramowitz and Stegun 1964).

8.2 Small $|z|$

Based on the definition of $z = (b_2 + a_2x)b_1/a_2^2$, this could occur in two cases: either at some finite interval in the strike space $|a_2| \gg |b_1x|$, $|a_2| \gg |b_2|$, or just z is small, so b_2 and a_2 have the opposite signs. In any case we have a small parameter under the high-order derivative. This equation belongs to the class of singularly perturbed differential equations (Wasow 1987). It can be solved by using either the method of matching asymptotic expansions (Nayfeh 2000), or the method of boundary functions (Vasil'eva et al. 1995). The latter was used in Itkin and Lipton (2018) in a similar situation, so for further details we refer a reader to that paper.

However, we can partly eliminate this by constructing solutions of (53) using the original variable x . Then we have to consider various cases where instead of a small parameter z some other combinations of parameters could be small or large. But if so, a general solution as a function of the original independent variable x could be represented as regular series on the new small parameter. Then, truncating the series, one gets a simplified solution.

To make it more transparent let us represent the general solution of (53) expressed in variable x , rather than in z , as this was done in (55)

$$V(x) = C_{j,i}^{(1)} y_1(x) + C_{j,i}^{(2)} y_2(x) + I_{12}(x),$$

$$y_i(x) = a_2^k (b_2 + a_2x)^k \mathcal{V}_i\left(-1 - \frac{b_0}{b_1} + \frac{b_1 b_2}{a_2^2}, 2 - \frac{b_1 b_2}{a_2^2}, \frac{b_1}{a_2^2} (b_2 + a_2x)\right), \quad i = 1, 2.$$

$$k = 1 - \frac{b_1 b_2}{a_2^2}.$$
(74)

Observe, that based on the definition of b_1 in (50), $b_1 \approx (r - q)\Delta T$, so usually small. Therefore, small z doesn't mean that w is necessarily small. Below we consider two cases.

8.2.1 $w \ll 1$

As $|z| \ll 1$ and $w \ll 1$ we have $w \ll |a_2^2/b_1|$. So $a_2 \geq \sqrt{b_1}$. In this case $w \ll 1$ is an actual small argument. Therefore, the general solution (74) can be expanded into series on small w . The condition $0 < w \ll 1$ implies that a_2 and b_2 have the opposite signs. If $a_2 > 0$ (and so $b_2 < 0$), then in the zero-order approximation we obtain

$$\begin{aligned}
 y_1(w) &= (a_2 w)^{k-1} \left[\frac{\Gamma(-k)}{\Gamma(b_0/b_1)} a_2 w + O(w^2) \right] \\
 &\quad - \left(\frac{b_1}{a_2^3} \right)^{1-k} \frac{\Gamma(k-1)}{b_1 \Gamma(k+b_0/b_1)} (a_2 b_1 b_2 - b_0 a_2 w) + O(w^2), \\
 y_2(w) &= (a_2 w)^{k-1} [a_2 w + O(w^2)].
 \end{aligned} \tag{75}$$

As $b_1 > 0$ we have $k - 1 > 0$.

If $a_2 < 0$ and $b_2 > 0$, then both RHS in (75) should be multiplied by a factor $\exp(-2i\pi b_1 b_2/a_2^2)$.

8.2.2 $a_2^2 \gg |b_1 w|$

In this case we can also expand the solution in (74) into series on small z to obtain

$$\begin{aligned}
 y_1(z) &= \frac{1}{\Gamma(1+q_1-q_2)} [\Gamma(1-q_2) - q_1 \Gamma(-q_2)z] + z^{-q_2} \left[\frac{\Gamma(q_2-1)}{\Gamma(q_1)} z + O(z^2) \right] + O(z^2), \\
 y_2(w) &= 1 + \frac{q_1}{q_2} z + O(z^2).
 \end{aligned} \tag{76}$$

Note, that based on the definition $q_2 = b_2 b_1/a_2^2$, at large a_2 the coefficient q_2 could also be small. But $z/q_2 = 1 + a_2 x/b_2 = w/b_2 = O(1)$.

9 Numerical Experiments

In our numerical test we use the same data set as in Itkin (2015); Itkin and Lipton (2018). This is done first, to compare performance and a quality of the fit for all those models. Also, we already know that these smiles are difficult to fit precisely, see discussions in Itkin (2015); Itkin and Lipton (2018).

To remind, we take data from <http://www.optionseducation.org> on XLF traded at NYSEArca on March 25, 2014. The spot price of the index is $S = 22.64$, and $r = 0.0148$, $q = 0.01$. The option implied volatilities (I_{call} , I_{put}) are given in Tables 2 and 3. We take all OTM quotes and some ITM quotes which are very close to the at-the-money (ATM). When strikes for Calls and Puts coincide, we take an average of I_{call} and I_{put} with weights proportional to $1 - |\Delta|_c$ and $1 - |\Delta|_p$ respectively, where Δ_c , Δ_p are option Call and Put deltas ⁶.

We have already mentioned that in our model for each term the slopes of the smile at plus and minus infinity, v_{j,n_j}^1 and $v_{j,0}^1$, are free parameters. So often traders

⁶ By doing so we do take into account effects reported in Ahoniemi (2009), who pointed out that the IVs calculated from Call and Put option prices corresponding to the same strike do not coincide, although they should be equal in theory. Our weights are chosen according to a pure empirical rule of thumb, and a more detailed investigation of this effect is required.

Table 2 XLF implied volatilities for the Put options

T	K _t Put	10	11	12	13	14	15	16	17	18	19	19.5	20	20.5	21	21.5	22	23
4/4/2014													39.53		23.77	19.73	16.67	
4/11/2014												35.89	30.33	26.62	22.06	18.49	16.11	
4/19/2014											32.90		26.79		20.14		15.19	12.93
5/17/2014									37.66	33.27	26.88		23.08		18.94		16.12	13.86
6/21/2014							40.51	37.21	31.41	27.84	23.90		21.07		18.88		16.95	15.82
7/19/2014							36.71	33.35	29.96	26.09	22.81		20.29		18.13		16.30	14.93
12/20/2014						31.98	29.38	27.21	25.30	23.75	22.09		20.67		19.44		18.36	17.60
1/17/2015	42.75	38.79	35.60	33.26	30.94	28.82	26.52	24.96	23.12	21.67			20.29		19.10		17.90	18.07

Table 3 XLF implied volatilities for the Put options

T	K, Call													
	21	21.5	22	22.5	23	23.5	24	25	26	27	28	29	30	
4/4/2014		16.60	14.69	14.40	14.86									
4/11/2014		16.89	14.96	14.52	14.77	14.98								
4/19/2014			15.79		13.38		15.39							
5/17/2014	16.71		14.48				13.75							
6/21/2014	16.31		14.78				13.92	14.28	16.58					
7/19/2014	16.82		15.24				14.36	14.19	15.20					
12/20/2014	17.63		16.61				15.86	15.47	15.12	15.18	15.03			
1/17/2015					16.95		17.25	16.23	15.73	15.50	15.58	15.86	16.47	

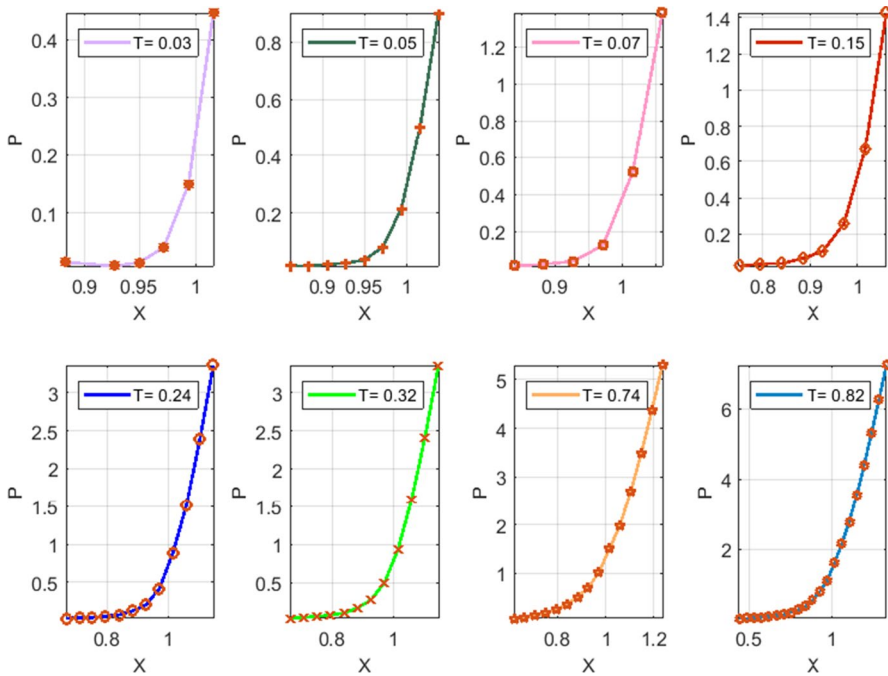


Fig. 5 Term-by-term fitting of market Put prices constructed using the whole set of data in Tables 2 and 3

have an intuition about these values. However, in our numerical experiments we take for them just some plausible values. In more detail, for a normalized variance $v(x)$ defined in (50), for all smiles we use $v_{j,0}^1 = -0.1$, and $v_{j,n_j}^1 = 0.1$. Accordingly, for the instantaneous variance $\sigma^2(x) = 2S^2v(x)/p_j$ the slopes at both zero and plus infinity are time-dependent and can be computed by using the above formula.

When calibrating the model to market data, we use the standard Matlab *fsolve* function, and utilize a “trust-region-dogleg” algorithm (see Matlab documentation on *fsolve*). Parameter “TypicalX” has to be chosen carefully to speedup calculations.

The results of this calibration which is done term-by term, are given in Fig. 5. Here each subplot corresponds to a single maturity T (marked in the legend) and shows market data (discrete points) and computed values (solid line). It can be seen that this simple local calibration algorithm provides a very accurate fit for all terms⁷.

We constructed the calibration algorithm to be smart enough in a sense that based on the values of parameters at each iteration it decides itself which particular solution (full or asymptotic) should be used at this iteration. We also observed that all full and asymptotic solutions are utilized by the algorithm when calibrating these market smiles.

⁷ Note, that in Itkin and Lipton (2018) in the last subplot the fit is not perfect in the vicinity of $X = -0.5$, where $X = \log K/F$ and $F = Se^{(r-q)T}$.

Table 4 Performance characteristics of the algorithm in the described experiment

Term	T (years)	Elapsed time (s)	Iterations	Function evaluations	Strikes
1	0.0274	0.86	97	1202	6
2	0.0466	2.83	97	1808	9
3	0.0685	1.43	95	1200	6
4	0.1452	0.64	48	433	8
5	0.2411	0.90	37	470	12
6	0.3178	2.98	82	1523	12
7	0.7397	6.60	106	3017	15
8	0.8164	149.67	56	1317	21

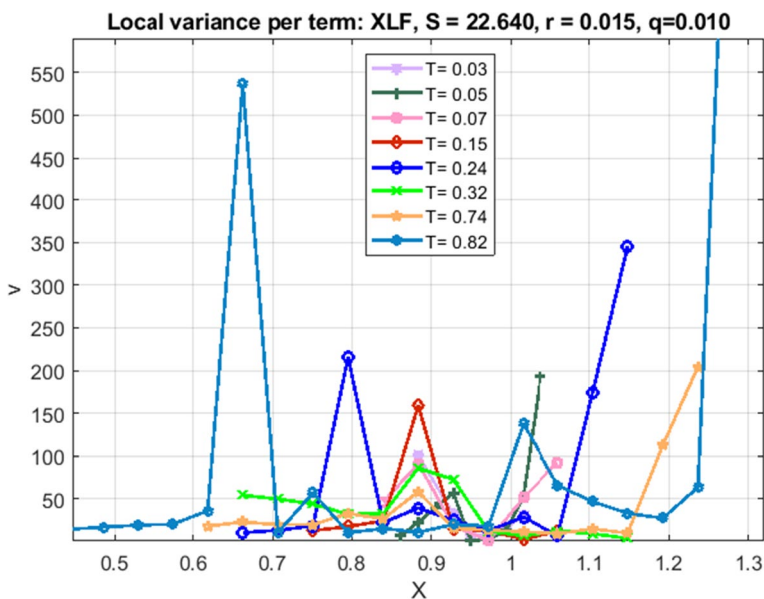
**Fig. 6** Term-by-term fitting of the instantaneous local variance $\sigma^2(x, T)$

Table 4 presents some performance measures of our algorithm. It can be seen that the elapsed time depends on the number of iterations and function evaluations necessary to converge to the given tolerance (we use a relative tolerance $\varepsilon = 10^{-4}$). This, in turn, depends on the number of evaluated Kummer functions (for the full solution), or number of exponential and Gamma functions (for the asymptotic solutions). Of course, the asymptotic solutions are much faster to evaluate, therefore an average time to calibrate a typical term is less than a second. For the last term 8 in Table 4 calibration is slow for two reasons: i) full solution is used based on the values of parameters, and 2) the number of strikes is higher than for the other terms. But the main reason is that the market data for this term is quite irregular. In

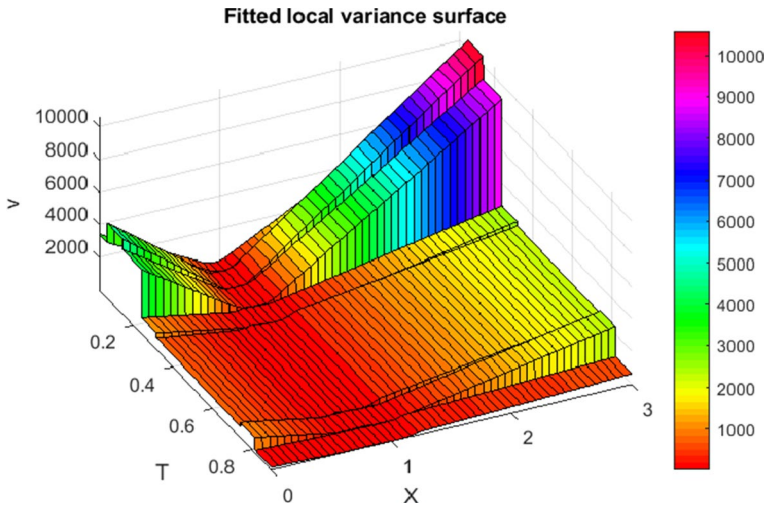


Fig. 7 The instantaneous local variance surface $\sigma^2(x, T)$ constructed by using the proposed approach

any case, performance of this model is much better than that reported in both Itkin (2015) and Itkin and Lipton (2018).

The local variance curves obtained as a result of this fitting are given term-by-term in Fig. 6. The corresponding local variance surface is represented in Fig. 7

By comparing the surface with that given in Itkin and Lipton (2018), one can notice that the shape is quite different while for calibration we use the same market smiles. This is because in Itkin and Lipton (2018) the standard local volatility model is used, where the underlying price follows a Geometric Brownian motion equipped with an instantaneous local volatility function, while in this paper the model is quite different.

To look at a more regular surface, we proceed with another example which is taken from Balaraman (2016). In that paper an implied volatility surface of S&P500 is presented, and the local volatility surface is constructed using the Dupire formula. In our test we take data for the first 12 maturities and all strikes as they are given in Balaraman (2016), and apply our model to calibrate the local variance surface as this is described in above. When doing so we set $v_{j,0}^1 = -0.3$, and $v_{j,n_j}^1 = 0.1$ for all smiles.

The results of this calibration are presented in Figs. 8, 9 and 10. By construction, our surface preserves no-arbitrage, while for the approach in Balaraman (2016) they have to solve some additional problems⁸.

⁸ As this is mentioned in Balaraman (2016), the correct pricing of local volatility surface requires an arbitrage free implied volatility surface. If the input implied volatility surface is not arbitrage free, this can lead to negative transition probabilities and/or negative local volatilities and can give rise to mispricing.

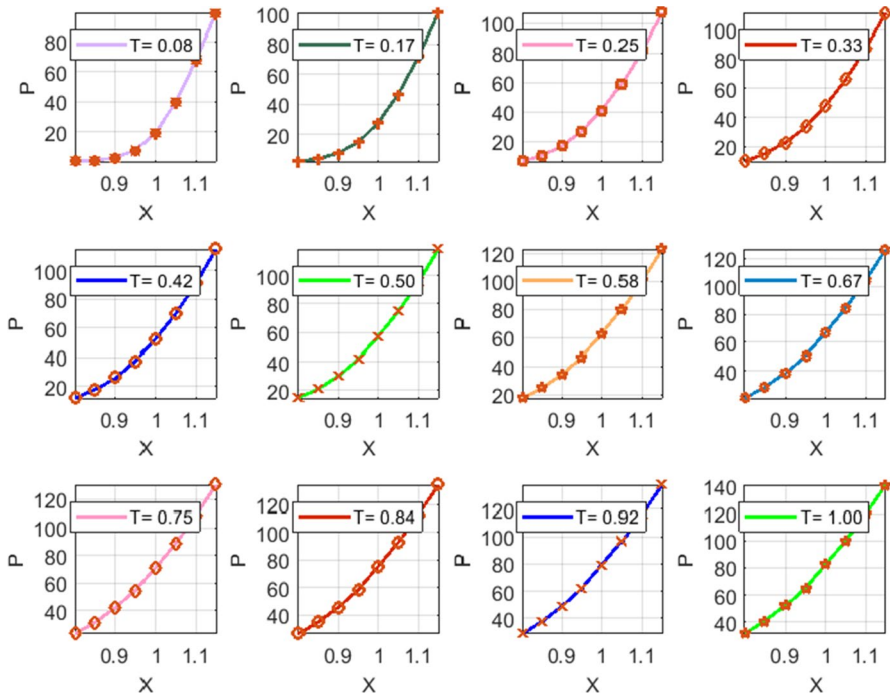


Fig. 8 Term-by-term fitting of market S&P500 Put prices constructed using data of Balaraman (2016)

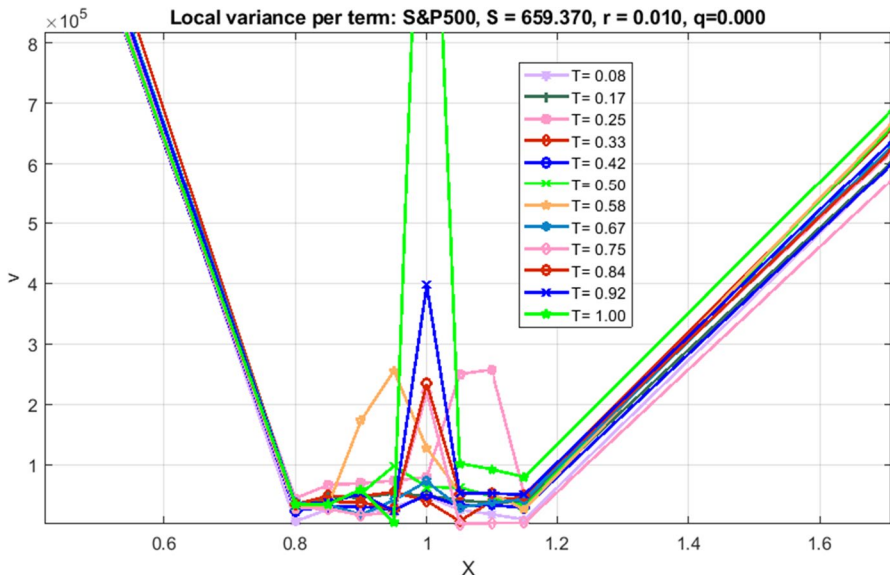


Fig. 9 Term-by-term fitting of the instantaneous local variance $\sigma^2(x, T)$ for S&P500

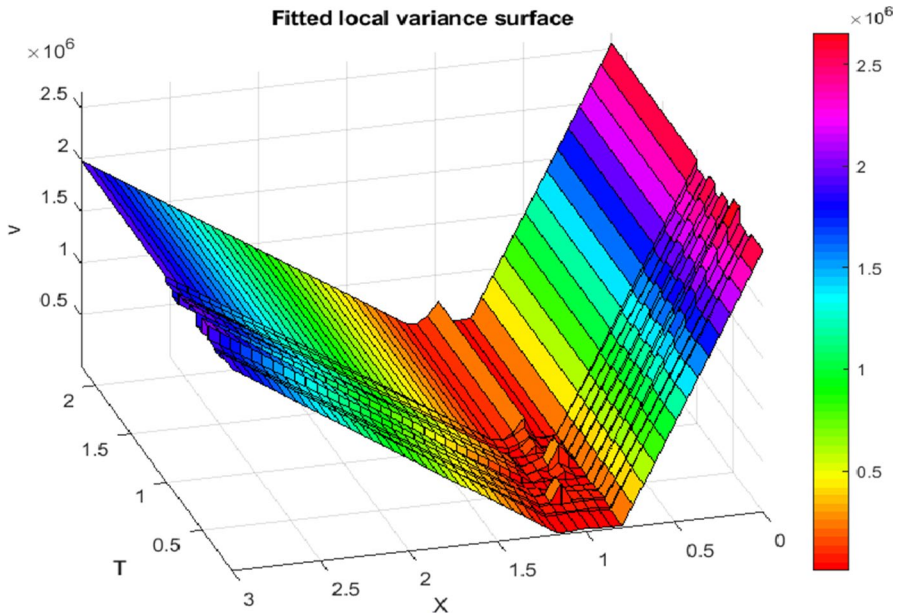


Fig. 10 The instantaneous local variance surface $\sigma^2(x, T)$ for S&P500 constructed by using the proposed approach

Table 5 Performance characteristics of the algorithm for calibration of a S&P500 surface

Term	T (years)	Elapsed time (s)	Iterations	Function evaluations	Strikes
1	0.0822	1.09	99	1604	8
2	0.1671	0.56	40	377	8
3	0.2521	2.32	94	1615	8
4	0.3315	1.70	97	1186	8
5	0.4164	0.10	15	64	8
6	0.4986	2.35	111	1600	8
7	0.5836	2.40	111	1584	8
8	0.6658	2.25	131	1604	8
9	0.7507	1.51	95	1072	8
10	0.8356	2.30	98	1603	8
11	0.9178	0.07	13	46	8
12	1.0027	72.80	74	795	8

In Table 5 we present the performance of our algorithm in this experiment. It can be seen that here the elapsed time is similar or shorter as compared with the previous test presented in Table 4.

10 Conclusions

In this paper we propose an expanded version of the Local Variance Gamma model of Carr and Nadtochiy (2017) which we refer as an Expanded Local Variance Gamma model, or ELVG. Two main improvements are introduced as compared with the LVG model. First, we add drift to the governing underlying process. It turns out that this a relatively minor (at the first glance) improvement requires a interesting trick to preserve tractability of the model, which is a non-trivial time-change. We show that still in this new model it is possible to derive an ordinary differential equation for the option price which plays a role of Dupire's equation for the standard local volatility model.

The second novelty of the paper as compared with the LVG model is that in contrast to Carr and Nadtochiy (2017) we consider a local variance to be a piecewise linear function of strike, while in Carr and Nadtochiy (2017) it was piecewise constant. We proceed in the spirit of Itkin and Lipton (2018) by describing a no-arbitrage interpolation, and then construct a closed-form solution of our ODE in terms of hypergeometric and generalized hypergeometric functions. An important advantage of this approach is that calibration of the model to market smiles does not require solving any optimization problem, and can be done term-by-term by solving a system of non-linear algebraic equations for each maturity. This is much faster than calibration of the local volatility model where to construct the objective function the optimizer needs the solution of the Dupire PDE. The speedup is pronounced, especially since we provide an algorithm for constructing a smart initial guess. We also provide various asymptotic solutions which allow a significant acceleration of the numerical solution and improvement of its accuracy in the corresponding cases (i.e., when parameters of the model at some iteration obey the conditions to apply the corresponding asymptotic).

In principle, somebody could claim that solving a system of nonlinear equations with a generic solver is not much different from solving a nonlinear optimization problem. Obviously, when our ODE is used as an alternative to the Dupire equation, the difference comes from the fact that calibration based on the Dupire equation requires solving this PDE at every iteration by either numerically, or semi-analytically by using a Laplace transform, which is obviously slower. As was mentioned in Introduction there exist many other calibration algorithms which reduce to a nonlinear optimization problem (e.g., taking a sufficiently large parametric family of local volatility functions and choosing the parameters that provide the best fit of observed prices). For the latter computation of the objective function is fast, but optimization must be constrained to preserve no-arbitrage, and, thus, slow.

In our numerical test we use same market data as in Itkin (2015); Itkin and Lipton (2018). The results of the test demonstrate robustness of the proposed approach from both the speed and accuracy point of view, especially in cases where the above referred papers experienced some difficulties with achieving a perfect fit. An additional test performed for the S&P500 data taken from Balaraman (2016) gives rise to the same conclusion.

References

- Abramowitz, M., & Stegun, I. (1964). *Handbook of mathematical functions*. Mineola: Dover Publications Inc.
- Ahoniemi, K. (2009). Modeling and forecasting implied volatility, Ph.D. thesis, Helsinki School of Economics.
- Balaraman, G. (2016). Modeling volatility smile and Heston model calibration using QuantLib python. Available at <http://gouthamanbalaraman.com/blog/volatility-smile-heston-model-calibration-quantlib-python.html>.
- Bergomi, L. (2016). *Stochastic Volatility Modeling, CRC Financial Mathematics Series*. London: Chapman and Hall.
- Bochner, S. (1949). Diffusion equation and stochastic processes. In *Proceedings of the National Academy of Sciences, USA* (Vol. 35, pp. 368–370).
- Carr, P., & Nadtochiy, S. (2014). Local variance gamma and explicit calibration to option prices. Available at [arXiv:1308.2326](https://arxiv.org/abs/1308.2326).
- Carr, P., & Nadtochiy, S. (2017). Local Variance Gamma and explicit calibration to option prices. *Mathematical Finance*, 27, 151–193.
- Coleman, T., Kim, Y., Li, Y., & Verma, A. (2001). Dynamic hedging with a deterministic local volatility function model. *The Journal of Risk*, 4, 63–89.
- Cox, J., & Rubinstein, M. (1985). *Options markets*. Upper Saddle River: Prentice-Hall.
- Derman, E., & Kani, I. (1994). Riding on a smile. *Risk*, 7, 32–39.
- Dupire, B. (1994). Pricing with a smile. *Risk*, 7, 18–20.
- Ekström, E., & Tysk, J. (2012). Dupire's equation for bubbles. *International Journal of Theoretical and Applied Finance*, 15, 1250041–1250053.
- Falck, M., & Deryabin, M. (2017). Local variance gamma revisited. Available at https://papers.ssrn.com/sol3/papers.cfm?abstract_id=2659728.
- Hull, J. C. (1997). *Options, futures, and other derivative securities* (3rd ed.). Upper Saddle River, NJ: Prentice-Hall Inc.
- Itkin, A. (2015). To sigmoid-based functional description of the volatility smile. *North American Journal of Economics and Finance*, 31, 264–291.
- Itkin, A. (2017) Pricing derivatives under Lévy models, number 12. In *Pseudo-differential operators*, 1st Edn, Basel: Birkhauser.
- Itkin, A., & Lipton, A. (2018). Filling the gaps smoothly. *Journal of Computational Sciences*, 24, 195–208.
- Kienitz, J., & Wetterau, D. (2012). *Financial modelling: Theory, implementation and practice with MATLAB source.*, The Wiley finance series New York: Wiley.
- Levy, H. (1985). Upper and lower bounds of put and call option value: Stochastic dominance approach. *The Journal of Finance*, 40, 1197–1217.
- Lipton, A., & Sepp, A. (2011). Credit value adjustment in the extended structural default model. In *The Oxford handbook of credit derivatives*, Oxford University (pp. 406–463).
- Madan, D., Carr, P., & Chang, E. (1998). The variance gamma process and option pricing. *European Finance Review*, 2, 79–105.
- Madan, D., & Seneta, E. (1990). The variance gamma (V.G.) model for share market returns. *Journal of Business*, 63, 511–524.
- Nayfeh, A. H. (2000). *Perturbation methods*. New York: Wiley.
- Ng, E., & Geller, M. (1970). On some indefinite integrals of confluent hypergeometric functions. *Journal of Research of the National Bureau of Standards—B. Mathematical Sciences*, 74B, 85–98.
- Olver, F. (1997). *Asymptotics and special functions*. New York: AKP Classics.
- Polyanin, A., & Zaitsev, V. (2003). *Handbook of exact solutions for ordinary differential equations* (2nd ed.). Boca Raton: CRC Press Company.
- Revuz, D., & Yor, M. (1999). *Continuous martingales and Brownian motion* (3rd ed.). Berlin: Springer.
- Shreve, S. (1992). Martingales and the theory of capital-asset pricing. *Lecture Notes in Control and Information SCIENCES*, 180, 809–823.
- Vasil'eva, A., Butuzov, V., & Kalachov, L. (1995). *The boundary function method for singular perturbation problems.*, Studies in applied mathematics Philadelphia: SIAM.

Wasow, W. (1987). *Asymptotic expansions for ordinary differential equations*. Mineola: Dover Publications.

Publisher's Note Springer Nature remains neutral with regard to jurisdictional claims in published maps and institutional affiliations.